IRWIN AND JOAN JACOBS
CENTER FOR COMMUNICATION AND INFORMATION TECHNOLOGIES

Blind Separation of Time / Position Varying Mixtures

Ran Kaftory and
Yehoshua Y. Zeevi

CCIT Report #758
February 2010

Electronics
Computers
Communications

DEPARTMENT OF ELECTRICAL ENGINEERING
TECHNION - ISRAEL INSTITUTE OF TECHNOLOGY, HAIFA 32000, ISRAEL

Blind Separation of Time/Position Varying Mixtures

Ran Kaftory and Yehoshua Y. Zeevi

Abstract

We address the fascinating open engineering problem of blindly separating time/position varying mixtures, and attempt to separate the sources from such mixtures without having prior information about the sources or the mixing system. Unlike studies concerning instantaneous or convolutive mixtures, we assume that the mixing system (medium) is changing in time/position. Attempts to solve this problem have mostly utilized, so far, online algorithms based on tracking the mixing system by methods previously developed for the instantaneous or convolutive mixtures. In contrast with these attempts, we develop a batch algorithm in the form of Staged Sparse Component Analysis (SSCA). Accordingly, we assume that the sources are either sparse or can be 'sparsified'. In the first stage we estimate the mixing system filters, based on the scatter plot of the sparse mixtures' data, using a proper grouping and curve/surface fitting. In the second stage, the mixing system is inverted, yielding the estimated sources. We use the SSCA approach for solving three types of mixtures: time/position varying instantaneous mixtures, single-path mixtures and multi-path mixtures. Real image mixtures and simulated mixtures are used to test our approach.

Index Terms

Blind Source Separation (BSS), Sparse Component Analysis (SCA), Time/Position Varying Mixing/Unmixing.

I. Introduction

Extensive research has been devoted over the last two decades to the subject of blind source separation (BSS), especially in the form of independent component analysis (ICA). The research mainly focused on the stationary, instantaneous and convolutive theoretical aspects of the problem and on practical applications. In the relevant models, the sources are attenuated by a fixed factor, and/or filtered by a fixed filter prior to being mixed. The approaches and techniques, used for solving the BSS problem of stationary mixtures, can be roughly divided into two categories: ICA and sparse component analysis (SCA). ICA assumes that the sources are statistically independent and, therefore, utilizes separation cost functions based on the maximization of non-Gaussianity [1], negentropy [2], maximum likelihood [3], or minimization of the mutual information [4], [5], diagonalization of the cumulant tensor [6], non-linear decorrelation [7] and second order statistics [8]. Blind separation using SCA assumes that the sources are sparse or can be projected onto a space of sparse representations by using a proper transformation ('sparsification'). The sources need not be statistically independent, but one should be able to represent them differently in some domain (i.e. there are atoms in a dictionary or instances in time/position in which only one source is represented or active). This approach lends itself to a geometric interpretation of the mixing coefficients. The mixing matrix entries can thereby be retrieved from the scatter plot of the 'sparsified' mixtures [9].

In most real-life scenarios, the mixing system is not constant as in the instantaneous or convolutive model, but it is changing as a function of time or position. The attenuation of signals/images varies over time/positin thus creating time/positin varying instantaneous mixtures. The delay/shift or reverberation/blurring of a signal/image may also vary over time/position creating a time/position varying single/multi-path mixtures. Only few studies address this generalized BSS problem. Most of them use the ICA approach and assume a slow varying mixing system, thus, enabling the use of an adaptive version of the algorithms developed for the stationary cases. The very few batch algorithms which assume a

Manuscript received xx, 2009; revised xx , 2010.

The authors are with the Department of Electrical Engineering, Technion - Israel Institute of Technology, Technion City, Haifa, 32000, Israel, (e-mail: kaftoryr@tx.technion.ac.il; zeevi@ee.technion.ac.il)

faster varying mixing system, limit themselves to a specific model of the variation of the mixing system. Table. I summarizes the approaches adopted by researches in order to solve the BSS of time/position varying mixtures.

TABLE I
METHODS FOR BSS OF TIME/POSITION VARYING MIXTURES COVERED BY THE LITERATURE

Approach	**Problem**	**Type**	**Criteria and References**
ICA	Instantaneous	Online	NonGaussianity: [10] Maximum Likelihood: [11] Mutual Information: [12],[13],[14] Non-linear Decorrelation: [15] Minimizing prediction error: [16],[17] All criteria: [18],[19],[20],[21],[22]
		Batch	Min. Helmholtz energy: [23],[24],[25] Second Order Statistics: [26][a], [27][b]
	Single/Multi path	Online	Second Order Statistics: [28],[29],[30] Nonlinear Decorellation: [31] Mutual Information: [32],[33],[34] Maximum Likelihood: [35], [36],[37] All criteria: [18]
		Batch	Second Order Statistics: [38][c]
SCA	Instantaneous	Online	Tracking Angle Histogram: [39]
		Batch	—
	Single/Multi path	Online	—
		Batch	—

[a] Works only for periodically time-varying mixing matrix
[b] Works only for linearly time-varying mixing matrix
[c] Works only for stationary mixtures of Doppler shifted sources

In this paper, we extend and generalize the BSS problem to cases of time/position varying mixtures that have not been dealt with so far, by using a staged SCA (SSCA) approach with batch algorithm. This enables the separation of mixtures of a faster varying mixing system with arbitrary model of variations. Accordingly, we assume that the sources are either sparse or can be 'sparsified'. In the first stage we estimate the mixing system filters, based on the scatter plot of the sparse mixtures' data, using a proper grouping and curve/surface fitting. In the second stage, the mixing system is inverted yielding the estimated sources. We study the conditions which enable the application of the SSCA and test our approach on experimental and simulated data.

The paper is organized as follows: Section I introduces the problem formulation and outlines the three types of time/position varying mixtures which occur in real-life scenarios. Section II outlines the SSCA approach for separating time/position varying mixtures. We study the conditions which enable the use of the SSCA approach in Section III. Sections IV-VI, present the methods and results of applying our approach to experimental and simulated data of three types of mixtures. Concluding remarks are summarized in section VII.

II. PROBLEM FORMULATION

We consider the case of separating N_s sources from N_z linear time/position varying mixtures, where the number of the sources and mixture $N_s = N_z$ is small. We use the vector notation for the independent variables $\underline{\xi} = (\xi_1, ..., \xi_{N_\xi})$, $\underline{\xi}' = (\xi_1', ..., \xi_{N_\xi}')$, where N_ξ is the number of independent variables. Denoting $Z = \left[z_1(\underline{\xi}), ..., z_{N_z}(\underline{\xi})\right]$ as a vector of the observed mixtures, and $S = \left[s_1(\underline{\xi}), ..., s_{N_s}(\underline{\xi})\right]$ as a vector of the sources, the observed mixtures are generated from the sources by a linear time varying transformation:

$$Z = H \star S + \eta, \tag{1}$$

where

$$H = \begin{bmatrix} h_{11}(\underline{\xi}, \underline{\xi}') & \cdots & h_{1N_s}(\underline{\xi}, \underline{\xi}') \\ \vdots & h_{ij}(\underline{\xi}, \underline{\xi}') & \vdots \\ h_{N_z 1}(\underline{\xi}, \underline{\xi}') & \cdots & h_{N_z N_s}(\underline{\xi}, \underline{\xi}') \end{bmatrix},$$

is a matrix of the mixing system filters, η is some unknown noise and the symbol $\star$ is defined as follows:

Definition 1: The symbol $\star$ denotes an integral operator with multidimensional kernel function acting on a single or multi-variable function. This operator is used for representing the linear filtering of a signal with a time/position varying filter and composition of such time/position varying filters:

1) Filtering with a filter ($\star : \mathbb{R}^{2N_\xi} \star \mathbb{R}^{N_\xi} \to \mathbb{R}^{N_\xi}$):

$$h \star s \equiv \int_{-\infty}^{\infty} h(\underline{\xi}, \underline{\xi}') s(\underline{\xi}') d\underline{\xi}', \tag{2}$$

2) Composition of filters ($\star : \mathbb{R}^{2N_\xi} \star \mathbb{R}^{2N_\xi} \to \mathbb{R}^{2N_\xi}$):

$$g \star h \equiv \int_{-\infty}^{\infty} g(\underline{\xi}, \underline{\xi}'') h(\underline{\xi}'', \underline{\xi}') d\underline{\xi}'', \tag{3}$$

where $g(\underline{\xi}, \underline{\xi}')$ and $h(\underline{\xi}, \underline{\xi}')$ are time/position varying filters used for filtering N_ξ-dimensional signals.

Similar to the definition of [40], we distinguish between three types of time/position varying mixtures:

1) Time/position varying instantaneous mixtures:
In this case, only the attenuation of the signals varies over time/position. We also assume that the signals arrive at the sensors instantaneously (in the case of images, without position shifts) and that they do not reverberate, nor do they have multiple reflections. The mixing system filters are given explicitly as:

$$h_{ij}(\underline{\xi}, \underline{\xi}') = a_{ij}(\underline{\xi}) \delta(\underline{\xi} - \underline{\xi}'), \tag{4}$$

where δ is the Kronecker's delta, and $a_{ij}(\underline{\xi})$ is the time/position varying attenuation of the j^{th} source with respect to the i^{th} sensor. Using the definition of $h_{ij}(\underline{\xi}, \underline{\xi}')$, Eq. (1) produces the following results for the generation of the time/position varying instantaneous mixtures:

$$z_i(\underline{\xi}) = \sum_j a_{ij}(\underline{\xi}) s_j(\underline{\xi}) + \eta(\underline{\xi}). \tag{5}$$

2) Time/position varying single-path[1] mixtures:
In this case, the attenuation and the delay/position shift of the signals/images change over time/position. This creates the doppler effect or the zooming/streching of images. We assume in this case, as in the instantaneous case, the absence of reverberations/multi-path/blurring. The mixing system filters are given explicitly as:

$$h_{ij}(\underline{\xi}, \underline{\xi}') = a_{ij}(\underline{\xi}) \delta(d_{ij}(\underline{\xi}) - \underline{\xi}'), \tag{6}$$

[1] In some studies the term anechoic mixtures is used

where $d_{ij}(\underline{\xi})$ is the time/position varying delay/position shift of the j^{th} source with respect to the i^{th} sensor. Using the definition of $h_{ij}(\underline{\xi}, \underline{\xi}')$, Eq. (1) yields the following results for the generation of the time/position varying single-path mixtures:

$$z_i(\underline{\xi}) = \sum_j a_{ij}(\underline{\xi}) s_j(d_{ij}(\underline{\xi})) + \eta(\underline{\xi}). \tag{7}$$

3) Time/position varying multi-path[2] mixtures:
In this case, the attenuation, delay/position shift and reverberation/multi-path/blur may change over time where the function of h_{ij} is arbitrary.

Fig. 1 provides a graphical (visual) interpretation of the above three types of position varying mixtures. Two image sources are mixed using different mixing filters, $h_{ij}(x, x')$. In the instantaneous case, only the attenuation of each source image varies from left to right. In the single-path mixture, varying the position shift varies the scale of the images from left to right. In the case of multi-path mixtures, we use a variable low-pass filter, which blurs the image differently from left to right.

III. Staged Sparse Component Analysis (SSCA)

Without loss of generality, we consider a system of two mixtures, $z_1(\underline{\xi}), z_2(\underline{\xi})$, of two sources, $s_1(\underline{\xi}), s_2(\underline{\xi})$. One of the approaches to the BSS problem is the SSCA, which is based on the assumption that the sources are sparse. We adopt this approach for solving the time/position varying BSS problem as outlined in the sequel.

A. Preprocessing: 'Sparsification'

Sparse signals are defined as those signals whose value differs significantly from zero only in a few instances of time/position. The probability density function (PDF) of such signals is modelled as an exponential [9]. The joint distribution of uncorrelated sparse signals is also approximately exponential. Therefore, if one source is active in some instance/position, the probability that the other source is 'active' in the same instance/position is very small. For signals which are not naturally sparse, a proper 'sparsification' transformation which is invariant to the mixing matrix can be applied.
'Sparsification' is defined as follows:

Definition 2: 'Sparsification' of a signal $s(\underline{\xi})$ is the process of applying a transformation T to the non-sparse signal $s(\underline{\xi})$ and yeilds a sparse output $T\left[s(\underline{\xi})\right]$.
We define invariancy of the 'sparsification' transformation to the mixing matrix as follows:

Definition 3: A 'sparsification' transformation T is invariant under mixing by the matrix, H, if

$$T\left[H \star S\right] = H \star T\left[S\right]. \tag{8}$$

The preprocessing required, according to the SSCA approach, implements an invariant sparsification transformation on both sides of Eq. (1), yielding the following separation problem:

$$T\left[Z\right] = H \star T\left[S\right]. \tag{9}$$

B. First Stage of the Separation Process: Mixing Matrix Estimation

In the noiseless case, all the time/position instances wherein the first sparsified source is active and the other is not-active satisfy the relations:

$$T[z_1] = h_{11} \star T[s_1], \qquad T[z_2] = h_{21} \star T[s_1]. \tag{10}$$

We define the new position-varying filter, g_1 such that:

$$T[z_2] = g_1 \star T[z_1]. \tag{11}$$

[2]In some studies the term echoic mixtures is used

Eq. (10) and Eq. (11) yield

$$h_{21} = g_1 \star h_{11}. \tag{12}$$

Similarly, for all the time/position instances in which the second sparsified source is active and the other is not, we define g_2 as $T[z_2] = g_2 \star T[z_1]$ and obtain $h_{22} = g_2 \star h_{12}$.

Even for the noisy case, it is possible to filter the time/position instances (usually by introducing some threshold) over which one of the sources can be regarded as active with respect to the not-active source, and where the noise is negligible [3]. The filters g_1 and g_2 are found by using a scatter plot of the sparse mixtures' data. A proper method of grouping/clustering these time/position instances and curve/surface estimation is used to estimate g_1 and g_2 out of the these active/not-active time/position samples of $T[z_1]$ and $T[z_2]$.

The first step of the SSCA is completed by substituting h_{21} and h_{21} for $g_1 \star h_{11}$ and $g_2 \star h_{12}$. This yields the following BSS problem:

$$\begin{aligned} T[z_1] &= h_{11} \star T[s_1] + h_{12} \star T[s_2] + \eta_1 \\ T[z_2] &= (g_1 \star h_{11}) \star T[s_1] + (g_2 \star h_{12}) \star T[s_2] + \eta_2. \end{aligned} \tag{13}$$

Using the associativity property of the operator $\star$ yields:

$$\begin{aligned} T[z_1] &= h_{11} \star T[s_1] + h_{12} \star T[s_2] + \eta_1 \\ T[z_2] &= g_1 \star (h_{11} \star T[s_1]) + g_2 \star (h_{12} \star T[s_2]) + \eta_2. \end{aligned} \tag{14}$$

Denoting $s_1' \equiv h_{11} \star s_1$ and $s_2' \equiv h_{12} \star s_2$, and recalling the invariancy property of the sparsification operator, Eq. (14) is rewritten as:

$$\begin{aligned} T[z_1] &= T[s_1'] + T[s_2'] + \eta_1 \\ T[z_2] &= g_1 \star T[s_1'] + g_2 \star T[s_2'] + \eta_2, \end{aligned} \tag{15}$$

or in the context of the vector notation of Eq. (1):

$$T[Z] = H' \star T[S'] + \eta, \tag{16}$$

where

$$H' = \begin{bmatrix} \boldsymbol{1} & \boldsymbol{1} \\ g_1 & g_2 \end{bmatrix},$$

and $\boldsymbol{1}$ is the identity filter which is defined as: $\boldsymbol{1} \equiv \delta(\underline{\xi} - \underline{\xi}')$.

We conclude this exposition with the analysis of a closely related BSS problem, in which the mixing filters have already been estimated (i.e. g_1 and g_2). The sources are not s_1 and s_2 but are s_1' and s_2', where the latter versions of s_1 and s_2 are filtered by the time/position varying filters h_{11} and h_{12} respectively. It is proven in [41] that this is the upper bound on the quality of estimating the sources.

C. Second Stage of the Separation Process: Solving the Inverse Problem

The task of the second stage of the SSCA is to solve the inverse problem of $Z = H' \star S' + \eta$, and estimate the sources. A 'naive' approach would be to directly invert the system:

$$\hat{S}' = H'^{-1} \star Z, \tag{17}$$

where

$$H'^{-1} \equiv (g_1 - g_2)^{-1} \star \begin{bmatrix} g_2 & -\boldsymbol{1} \\ -g_1 & \boldsymbol{1} \end{bmatrix}.$$

[3] After the sparsification preprocessing the SNR is improved

However, matrix inversion and the calculation of the determinant is feasible only for commutative rings, which is not the general case of sets of time/position varying filters. Even for a subset of time/position varying filters, which commute, direct inversion requires the inversion of the difference filter $g_1 - g_2$. This filter can be singular or badly conditioned, in which case, its inverse amplifies the noise and yields noisy estimation of the image sources. To overcome this problem we use a variational method which is effective in both cases of noncommutative mixing time/position varying filters and singular or badly conditioned mixing matrix. Instead of inverting the system, a cost function is defined:

$$\mathbb{J} = \|Z - H' \star \hat{S}'\| + w\mathbf{R}(\hat{S}'), \tag{18}$$

where $\mathbf{R}(\cdot)$ is a regularization operator and w is a weighting parameter. The minimization of this cost function using the Euler-Lagrange equations yields an estimation of the separated sources.

IV. Conditions Which Enable the Use of the SSCA

In order to successfully apply the SSCA approach in separation of time/position varying mixtures, proper conditions must be fulfilled. In this section, we outline the conditions which concern the sparsity of the sources signals, signal-to-noise ratio, the mixing filters, sparsification transformation and the filter matrix.

A. Conditions on the Noise and Signal Sources

The first step of the SSCA requires to filter time/position instances where one sparsified source is active while the others are not, and the noise is negligible. In the sequel we show that for 'sparsified' sources this probability increases as the value of the observed mixture increases. We define the following criteria for the above specified instances.

Definition 4: A time/position instance $\underline{\xi}_0$ in which one sparsified source can be regarded as active and the other is not is defined as follows:

$$\left|\frac{h_{i1} \star T[s_1(\underline{\xi}_0)]}{h_{i2} \star T[s_2(\underline{\xi}_0)]}\right| > th_1, \tag{19}$$

where the ratio on the left hand side is termed Contributing-Signal-to-Interfering-Signal Ratio (CSISR) and the right hand side is a subjective threshold which depends on the robustness of the algorithm for estimating the mixing filters as well as the mixing filters themselves.

Definition 5: A time/position instance $\underline{\xi}_0$ in which the sparsified noise is negligible with respect to the mixture of the two 'sparsified' sources is defined as:

$$\left|\frac{h_{i1} \star T[s_1(\underline{\xi}_0)] + h_{i2} \star T[s_2(\underline{\xi}_0)]}{T[\eta_i]}\right| > th_2, \tag{20}$$

where the ratio on the left hand side is termed Contributing Signals-to-Noise Ratio (CSNR) and the right hand side is a subjective threshold which depends on the robustness of the algorithm for estimating the mixing filters as well as the mixing filters themselves.

The probability density function (PDF) of a sparsified source is modelled as an exponential [42], $pdf(T[s]) = ke^{-\mu|T[s]|^{1/\nu}}$, where μ is a positive parameter, $\nu \geq 1$, and $k = (\int\limits_{-\infty}^{\infty} e^{-\mu|T[s]|^{1/\nu}})^{-1}$ is a normalization parameter [9].

We assume that the noise is not sparse even after applying the sparsification transformation. Therefore, we can assume that the PDF of the noise is Gaussian with zero mean and some standard deviation: $pdf(T[\eta]) = ke^{-\frac{T[\eta]^2}{2\sigma^2}}$, where σ is the standard deviation of the noise and $k = \frac{1}{\sqrt{2\pi\sigma}}$ is a normalization parameter.

Proposition 1: The conditional probability that one sparsified source is active and the other is not, where the noise is negligible in some time/position instance $\underline{\xi}_0$, given the observed sparsified mixture $T[z_i(\underline{\xi}_0)]$, and the thresholds th_1, and th_2, is:

$$p\left(CSISR > th_1, CSNR > th_2 \mid T[z_i] = T[z_i(\underline{\xi}_0)]\right) =$$

$$= \frac{\int\limits_{m_1}^{m_2}\int\limits_{l_1}^{l_2} e^{-\frac{(T[z_i(\underline{\xi}_0)]-\underline{\zeta})^2}{2\sigma^2} - |\underline{\zeta}-\underline{\phi}|^{1/\nu_{i1}}\mu_{i1}^T - |\underline{\phi}|^{1/\nu_{i2}}\mu_{i2}^T} d\underline{\phi}d\underline{\zeta}}{\int\limits_{-\infty}^{\infty}\int\limits_{-\infty}^{\infty} e^{-\frac{(T[z_i(\underline{\xi}_0)]-\underline{\zeta})^2}{2\sigma^2} - |\underline{\zeta}-\underline{\phi}|^{1/\nu_{i1}}\mu_{i1}^T - |\underline{\phi}|^{1/\nu_{i2}}\mu_{i2}^T} d\underline{\phi}d\underline{\zeta}} +$$

$$+ \frac{\int\limits_{m_1}^{m_2}\int\limits_{l_3}^{l_4} e^{-\frac{(T[z_i(\underline{\xi}_0)]-\underline{\zeta})^2}{2\sigma^2} - |\underline{\zeta}-\underline{\phi}|^{1/\nu_{i1}}\mu_{i1}^T - |\underline{\phi}|^{1/\nu_{i2}}\mu_{i2}^T} d\underline{\phi}d\underline{\zeta}}{\int\limits_{-\infty}^{\infty}\int\limits_{-\infty}^{\infty} e^{-\frac{(T[z_i(\underline{\xi}_0)]-\underline{\zeta})^2}{2\sigma^2} - |\underline{\zeta}-\underline{\phi}|^{1/\nu_{i1}}\mu_{i1}^T - |\underline{\phi}|^{1/\nu_{i2}}\mu_{i2}^T} d\underline{\phi}d\underline{\zeta}}, \tag{21}$$

where for $\underline{\zeta} \geq 0$,

$$l_1 \equiv \frac{\underline{\zeta}}{1-th_1}, \quad l_2 \equiv \frac{\underline{\zeta}}{1+th_1}, \quad l_3 \equiv \frac{\underline{\zeta} th_1}{th_1+1}, \quad l_4 \equiv \frac{\underline{\zeta} th_1}{th_1-1},$$

and for $\underline{\zeta} < 0$, l_1 and l_2 are interchanged and so are l_3 and l_4.

If $z_i(\underline{\xi}_0) \geq 0$,

$$m_1 = \frac{T[z_i(\underline{\xi}_0)]th_2}{th_2+1}, \quad m_2 = \frac{T[z_i(\underline{\xi}_0)]th_2}{th_2-1},$$

and if $z_i(\underline{\xi}_0) < 0$, m_1 and m_2 are interchanged. (For a proof see the Appendix).

Fig. 2 depicts the conditional probability of sparsified signal distribution, with $\mu = 1.5$ and $\nu = 2$ plotted as a function of $T[z_i(\underline{\xi}_0)]$ for several values of σ. It is observed that the probability is a monotonic non non-decreasing function of $|T[z_i(\underline{\xi}_0)]|$. Therefore, as a rule of thumb, it is possible to use a proper threshold on the observed mixture such that the probability that only one source is active, and the noise is negligible, is high. In such instances, the estimation of the mixing filters is possible. The number of such instances which is required for the correct estimation of the mixing filter is discussed in reference to the context of conditions required for mixing filters estimation.

B. Conditions on the Mixing Filters

The first step of the SSCA approach, requires the existence of g_i and its estimation based on samples of the observed measurements. Assuming that g_i exists, we can obtain only samples of the filter using a threshold over which we can assume a high probability for only one source to be active, and the noise to be negligible. These samples are distributed randomly and depend on both the source signals and the noise. If we assume that we know the filter g_i up to some finite number N_k of unknown parameters, and the function is injective, then we need at least the same number (N_k) of samples of that filter, in order to obtain the unknown parameters. If the filter is unknown, a Taylor approximation can be derived using some N_k-order polynomial function:

$$\hat{g}_i(\xi_1, ..., \xi_{N_\xi}, \xi'_1, ..., \xi'_{N_\xi}) =$$

$$= \sum_{k_1=0}^{N_k} ... \sum_{k_{N_k}=0}^{N_k} \sum_{k'_1=0}^{N_k} ... \sum_{k'_{N_k}=0}^{N_k} \alpha_{k_1,...,k_{N_k},k'_1,...k'_{N_k}} \tag{22}$$

$$(\xi_1 - \xi_{1_0})^{k_1} \cdots (\xi_{N_\xi} - \xi_{N_{\xi_0}})^{k_{N_k}} (\xi'_1 - \xi'_{1_0})^{k'_1} \cdots (\xi'_{N_\xi} - \xi'_{N_{\xi_0}})^{k'_{N_k}}.$$

It takes $(N_k + 1)^{2N_\xi}$ samples to calculate the unknowns α parameters by the Lagrangian interpolation formula, [43].

A non-parametric approach for estimating g_i out of its samples would require the following condition:

Proposition 2: if $g_i(\underline{\xi}, \underline{\xi}')$ is band-limited to a region Ω, it can be uniquely represented by nonuniformly distributed samples satisfying the Nyquist rate, on the average, as long as the samples are not on the zero-crossing contours of any member of the set of all functions band-limited to Ω. [The proof for 1D and 2D functions is given in [44]].

In practice, the function g_i is usually known up to a finite number of parameters, using some prior knowledge regarding the physics of the mixing system. In other cases, it can be assumed that it is a smooth function and therefore band-limited to a small region Ω, which allows the use of a non-parametric function estimation by means of a low average sampling rate.

By definition, $g_1 = h_{21} \star h_{11}^{-1}$ and $g_2 = h_{22} \star h_{12}^{-1}$, therefore, the filters g_1 and g_2 exist only if h_{11}^{-1} and h_{12}^{-1} exist. We now provide the conditions for the existence of an inverse filter by using the frequency analysis of time/position varying systems.

Zadeh [45] was the first to present an approach suitable for the analysis of linear time-varying systems in the context of frequency analysis. His transform has rarely been used [46] but it is useful for our purposes. We consider the linear time/position varying system representation as the superposition integral: $z(\underline{\xi}) = h(\underline{\xi}, \underline{\xi}') \star s(\underline{\xi})$, where $h(\underline{\xi}, \underline{\xi}')$ is the system response at the instance $\underline{\xi}$ to the impulse $\delta(\underline{\xi} - \underline{\xi}')$.

Zadeh defined the frequency response of the time/position varying system, to a unit impulse applied at $\underline{\xi} = \underline{\xi}_0$ as:

$$\mathcal{H}_Z(\underline{\xi}_0, \underline{\omega}) = \int_{-\infty}^{\infty} h(\underline{\xi}_0, \underline{\xi}') e^{-j\underline{\omega}(\underline{\xi}_0 - \underline{\xi}')^T} d\underline{\xi}'. \tag{23}$$

The following Proposition, indicates that Zadeh's transform can be used for the synthesis of variable systems. The output of such a system to a given input can be found using the system frequency response.

Proposition 3: The output of the system $z(\underline{\xi}) = h(\underline{\xi}, \underline{\xi}') \star s(\underline{\xi})$ can be calculated using the system frequency response:

$$z(\underline{\xi}) = \frac{1}{2\pi} \int_{-\infty}^{\infty} \mathcal{H}_Z(\underline{\xi}, \underline{\omega}) \mathcal{S}_F(\underline{\omega}) e^{j\underline{\omega}\underline{\xi}^T} d\underline{\omega}, \tag{24}$$

where $\mathcal{S}_F(\underline{\omega})$ is the Fourier transform of $s(\underline{\xi})$: $\mathcal{S}_F(\underline{\omega}) = \int_{-\infty}^{\infty} s(\underline{\xi}) e^{-j\underline{\omega}\underline{\xi}^T} d\underline{\xi}$. (For the proof see the Appendix).

It is important to find the frequency response of a composition of time/position varying filters. The following Theorem provides the relations between the frequency response of a system to the frequency response of its components.

Lemma 4: The Zadeh frequency response of the system: $f = g \star h$, is given by the Zadeh frequency responses, $\mathcal{G}_Z(\underline{\xi}, \underline{\omega})$ and $\mathcal{H}_Z(\underline{\xi}, \underline{\omega})$ as:

$$\mathcal{F}_Z(\underline{\xi}, \underline{\omega}) = \sum_{i=0}^{n} \frac{1}{i!} \frac{\partial^i \mathcal{G}_Z(\underline{\xi}, \underline{\omega})}{\partial (j\underline{\omega})^i} \frac{\partial^i \mathcal{H}_Z(\underline{\xi}, \underline{\omega})}{\partial \underline{\xi}^i}, \tag{25}$$

where n is the order of the differential system representing the SISO system. (For a proof see [47]).

A condition establishing relationship between the Zadeh frequency responses of the filter and its inverse is defined by the following Theorem:

Theorem 5: The time/position varying filter $h(\underline{\xi}, \underline{\xi}')$ has an inverse $g(\underline{\xi}, \underline{\xi}')$ only if $\mathcal{G}_Z(\underline{\xi}, \underline{\omega})$, which is the Zadeh frequency response of $g(\underline{\xi}, \underline{\xi}')$, satisfies the equation:

$$\sum_{i=0}^{n} \frac{\partial^i \mathcal{G}_Z(\underline{\xi}, \underline{\omega})}{\partial (j\underline{\omega})^i} \frac{\partial^i \mathcal{H}_Z(\underline{\xi}, \underline{\omega})}{\partial \underline{\xi}^i} = 1, \tag{26}$$

where n is the order of the differential equation. [For a proof see the Appendix).

Therefore, the filters g_1 and g_2 exist only if h_{11}^{-1} and h_{12}^{-1} exist and fulfil Eq. (26), where h and g are substituted by h_{11} or h_{12} and h_{11}^{-1} or h_{12}^{-1}, respectively.

C. Conditions on the Sparsification Transformation

A sufficient condition for the existence of a sparsification transformation is its invariancy to the mixing matrix. We provide a weaker explicit condition sufficient for a subset of sparsification transformations, which can be regarded as filtering with a time/position varying filter: $T[H \star S] = T \star (H \star S)$.

Recalling Definition 3 with this subset of transformations, the invariancy to the mixing matrix means that $T \star (H \star S) = H \star (T \star S)$, or explicitly for a 2x2 mixing system:

$$T \star (h_{i1} \star s_1 + h_{i2} \star s_2) = h_{i1} \star (T \star s_1) + h_{i2} \star (T \star s_2) \,. \tag{27}$$

This implies that a transformation which is invariant to the mixing matrix should be commutative over the operator $\star$.

Proposition 6: The operator $\star$ along with the set of $2N_\xi$-dimensional time/position varying filters perform a noncommutative operation: $g \star h \neq h \star g$, where g and h are time/position varying filters. [For a proof see the Appendix].

Therefore, in general, by substituting g with T and h with h_{i1}, $T \star h_{i1} \neq h_{i1} \star T$. A similar non-commutative operation is obtained for h_{i2}. But, using the Zadeh transform, we can find the subset of transformations which do commute:

Corollary 7: The filters h and g commute, if their relative Zadeh frequency responses obey:

$$\begin{aligned} &\sum_{i=0}^{n} \frac{1}{i!} \frac{\partial^i \mathcal{G}_Z(\underline{\xi}, \underline{\omega})}{\partial (j\underline{\omega})^i} \frac{\partial^i \mathcal{H}_Z(\underline{\xi}, \underline{\omega})}{\partial \underline{\xi}^i} = \\ &= \sum_{i=0}^{n} \frac{1}{i!} \frac{\partial^i \mathcal{H}_Z(\underline{\xi}, \underline{\omega})}{\partial (j\underline{\omega})^i} \frac{\partial^i \mathcal{G}_Z(\underline{\xi}, \underline{\omega})}{\partial \underline{\xi}^i} . \end{aligned} \tag{28}$$

This result implies that filters which have a fixed-in-$\underline{\xi}$ Zadeh frequency response, commute with similar filters. Filters which have a fixed-in-$\underline{\omega}$ Zadeh frequency response, commute with similar filters (the proof follows directly from Theorem 4).
Therefore, the filters T and h_{i1} or h_{i2} commute if the condition of Eq. (28) is fulfilled by substituting g and h with T and h_{i1} or h_{i2}, respectively.

D. Conditions on the Mixing Matrix

The second step of the SSCA requires the solution of the inverse problem of $Z = H \star S$. It can be accomplished by means of Eq. (17) by using the inverse of H. However, matrix algebra which includes the calculation of the determinant and the inverse of a matrix, is defined only over a commutative ring. In our case, we show that in general, the set of $2N_\xi$-dimensional time/position varying filters together with addition and the operator $\star$ (which substitutes multiplication) constitute a noncommutative ring and, therefore, matrix algebra cannot be performed.

A ring of elements is defined with two binary operators: 'addition' and 'multiplication'. It requires the elements to constitute a commutative group over 'addition' and a monoid over 'multiplication'.

Theorem 8: The set of $2N_\xi$-dimensional time/position varying filters, and the two binary operators of addition and $\star$ (which serves as 'multiplication') constitute a non-commutative ring. (Proof is provided in the Appendix].

Nevertheless, it is possible to find a subset of $2N_\xi$-dimensional time/position varying filters which commute with each other, using Corollary 7. These filters are regarded as their centralizer, where the centralizer is defined as follows:

Definition 6: The centralizer of an element, h, of a monoid associated with the operator $\star$, is the set of all the elements g_i in that monoid which obey: $h \star g_i = g_i \star h$.

Therefore, matrix algebra can be performed for the subset of filters which costitute the centralizer of themselves. As a consequence, the inverse of a matrix can be calculated using the following Corollary:

Corollary 9: If the elements of H, a matrix of $N_z - by - N_s$, $N_z = N_s$ time/position varying filters, belong to the centralizer of the matrix filters, and if H is invertible then its inverse is given by:

$$H^{-1} = det(H)^{-1} \star \begin{bmatrix} c_{11} & \cdots & c_{1N_s} \\ \vdots & \ddots & \vdots \\ c_{N_z1} & \cdots & c_{N_zN_s} \end{bmatrix}, \tag{29}$$

where $det(H)^{-1}$ is the inverse filter of the determinant filter, which results from calculating $det(H)$, and c_{ij} is the matrix cofactor (this is proved by Cramer's rule of linear algebra).

As a result, a matrix of $N_z - by - N_z$ time/position varying filters, H, is invertible only if the determinant of H is invertible.

Nevertheless, the existence of H'^{-1} is a necessary condition for solving directly the inverse problem, but not sufficient. The matrix H can be ill-conditioned, meaning a small change in the input results in a large change of the output.

Looking at the inverse problem of the second stage in Eq. (16), we can observe that for the noisy case:

$$\begin{aligned} \begin{bmatrix} \hat{s'_1} \\ \hat{s'_2} \end{bmatrix} &= (g_1 - g_2)^{-1} \star \begin{bmatrix} g_2 & -\mathbf{1} \\ -g_1 & \mathbf{1} \end{bmatrix} \star \begin{bmatrix} z_1 \\ z_2 \end{bmatrix} = \\ = \begin{bmatrix} s'_1 \\ s'_2 \end{bmatrix} &+ (g_1 - g_2)^{-1} \star \begin{bmatrix} g_2 & -\mathbf{1} \\ -g_1 & \mathbf{1} \end{bmatrix} \star \begin{bmatrix} \eta_1 \\ \eta_2 \end{bmatrix} = \\ = &\begin{bmatrix} s'_1 + (g_1 - g_2)^{-1} \star g_2 \star \eta_1 - (g_1 - g_2)^{-1} \star \eta_2 \\ s'_2 - (g_1 - g_2)^{-1} \star g_1 \star \eta_1 + (g_1 - g_2)^{-1} \star \eta_2 \end{bmatrix}, \end{aligned} \tag{30}$$

where η_1 and η_2 are the noise in the respective sensors.

Therefore, if the filter $(g_1 - g_2)^{-1}$ or any of the composed filters $(g_1 - g_2)^{-1} \star g_2$ or $(g_1 - g_2)^{-1} \star g_1$ amplify the noise, the error of estimation due to the noise is large.

We assume that the noise η is a white Gaussian noise that results form a stationary stochastic process. Filtering such noise with a time/position varying filter results in a non-stationary process. Therefore, the error in estimating the sources can be small for some time/postition instances or large for others. In the Zadeh transform domain, we can state the following Proposition

Proposition 10: The time/position varying power spectral density of the white Gaussian noise filtered by the time/position varying filter $g(\underline{\xi}, \underline{\xi}')$ is $NSD|\mathcal{G}_Z(\underline{\xi}, \underline{\omega})|$, where NSD is the noise spectral density (the proof is given in [41]).

Consequently, amplification of the noise occurs whenever $|\mathcal{G}_Z(\underline{\xi}, \underline{\omega})| \geq 1$. The conditions for solving directly the inverse problem using the inverse of the mixing matrix H'^{-1} is therefore:

1) $|Z\{(g_1 - g_2)^{-1}\}| \geq 1$,
2) $|Z\{(g_1 - g_2)^{-1} \star g_1\}| \geq 1$,
3) $|Z\{(g_1 - g_2)^{-1} \star g_2\}| \geq 1$,

where $Z\{\cdot\}$ stands for the Zadeh frequency response. Whenever the conditions for solving directly the inverse problem are not fulfilled, the variational approach can be used.

In the following sections, we outline the methods and the results of applying our approach to experiments and simulated data for the three types of time/position varying mixtures. For each type, we outline the method for the sparsification of the mixtures, the method for estimating the mixing filters g_i out of the scatter-plot of the mixtures' data, the method for the inversion of the BSS problem to estimate the sources and when applicable, we describe a system for generating real mixtures. We also demonstrate results of separating the sources using experimental data and simulations.

V. Methods and Results for Blind Separation of Time/Position Varying Instantaneous Mixtures

For this section[4], we assume that the mixing filters have the form of Eq. (4). We also assume the following:

1) The model of the instantaneous mixing filters is arbitrary, but it is known up to a finite number of parameters.
2) Apart from some instances, the zero order Taylor approximation of the instantaneous mixing filters around some instance in a small window, is sufficient to represent the function in that window.
3) The sources are sparse or can be sparsely represented using an appropriate transform.

A. Sparsification Using Wavelet packets and Short Time Fourier Transform

The Zadeh transform of the mixing filters, h_{ij}, is as follows:

$$\begin{aligned}\mathcal{H}_{Z_{ij}}(\underline{\xi},\underline{\omega}) &= \int_{-\infty}^{\infty} a_{ij}(\underline{\xi})\delta(\underline{\xi}-\underline{\xi}')e^{j\underline{\omega}(\underline{\xi}-\underline{\xi}')^T}d\underline{\xi}' = \\ &= a_{ij}(\underline{\xi}). \end{aligned} \tag{31}$$

Observe that the Zadeh frequency response of the mixing filters is independent of $\underline{\omega}$. Therefore, using Corollary 7, every sparsification transformation which also has a Zadeh frequency response independent of $\underline{\omega}$, is an element of the centralizer. Elements of the centralizer commute with the mixing filter and are therefore invariant of the mixing matrix. Unfortunately, all the known linear sparsification transformations which can be written as a time/position varying filter, extract usually, the high frequencies of the signals. This implies that they have an $\underline{\omega}$-dependent frequency response and, therefore, are not members of the centralizer, nor are invariant to the mixing matrix.

Nevertheless, we can utilize the second assumption of this section and estimate the mixing filters over a small windows around some instances (where the assumption holds) as though they are fixed (in $\underline{\xi}$) filters. The Zadeh frequency response of such fixed filters is independent of $\underline{\xi}$ and therefore, using Corollary 7, every sparsification transformation which can be written also as a fixed (in $\underline{\xi}$) filter, is a member of the centralizer and, therefore, commutes and is invariant to the mixing matrix over these instances.

The short time Fourier transform (STFT) can be used for sparse representation of audio and other harmonic signals, whereas wavelet packets can be used for images [49]. The STFT window size, and the support of the filter in the wavelet packets decomposition, should follow the above assumption in order to produce an invariant transform.

B. Parametric Mixing Filters Estimation

We assume for the rest of this section, that the mixtures are of 1D signals. In the case of images, the columns are concatenated to form a single vector. If we group the instances, $\{\xi_l\}$, where one of the sources is active and the other is not, using some threshold, the values of g_i for these instances are according to Eq. (11):

$$g_i(\xi_l) \approx \frac{T[z_2(\xi_l)]}{T[z_1(\xi_l)]}. \tag{32}$$

As a result, the mixing filter g also has the form of $g_i(\xi,\xi') = a_i(\xi)\delta(\xi-\xi')$. According to the first assumption, the mixing filters are known up to a finite number of parameters, which means that: $a_i(\xi) \equiv a_i(\alpha_{i_k};\xi)$, where α_{i_k} are the unknown parameters.

We wish to construct a unified framework for grouping time/position instances originated from the same sensor for estimating the α_{i_k} parameters. This unified framework is necessary since correct estimation of α_{i_k} solves the grouping problem and vice versa. Correct grouping estimates the parameters α_{i_k}.

[4]Some of the methods and the results of this section were presented in [48]

Suppose that we take N_m time/position instances $\xi_0 ... \xi_{(N_m-1)}$ in which a signal was detected above the threshold. For each individual instance ξ_l, we define the ratio $r_i(\xi_l) \equiv T[z_i(\xi_l)]/T[z_1(\xi_l)]$.

A maximum likelihood approach for estimating α_{i_k} would be to maximize:

$$\arg\max_{\alpha_{i_k}} \mathbb{J}(\alpha_{i_k}) \equiv \arg\max_{\alpha_{i_k}} p(r_i(\xi_0 ... \xi_{(N_m-1)}) \mid \alpha_{i_k}). \tag{33}$$

Using Bayes' rule, we can calculate the conditional probability of Eq. (33) by:

$$\begin{aligned} & p(r_i(\xi_0 ... \xi_{(N_m-1)}) \mid \alpha_{i_k}) = \\ &= \frac{p(\alpha_{i_k} \mid r_i(\xi_0 ... \xi_{(N_m-1)})) p(r_i(\xi_0 ... \xi_{(N_m-1)}))}{p(\alpha_{i_k})}. \end{aligned} \tag{34}$$

Since prior information regarding the distribution of α_{i_k} is not available, a uniform distribution is assumed. Omitting $p(\alpha_{i_k})$, which is assumed to be constant, and omitting $p(r_i(\xi_0 ... \xi_{(N_m-1)}))$, which does not depend on α_{i_k}, does not affect the maximization of Eq. (34) with respect to α_{i_k}. Therefore, estimating α_{i_k} by using the maximum likelihood approach corresponds to maximizing

$$\arg\max_{\alpha_{i_k}} \mathbb{J}(\alpha_{i_k}) \equiv \arg\max_{\alpha_{i_k}} p(\alpha_{i_k} \mid r_i(\xi_0 ... \xi_{(N_m-1)})). \tag{35}$$

In order to evaluate the conditional probability $p(\alpha_{i_k} \mid r_i(\xi_0 ... \xi_{(N_m-1)}))$, we first construct a density estimation to get a certain ratio on a specific instance, given the measurements $T[z_i(\xi_l)]$ and $T[z_1(\xi_l)]$. It can be done using a kernel density estimation:

$$\begin{aligned} & \hat{f}(r_i, \xi \mid T[z_i(\xi_l)], T[z_1(\xi_l)]) = \\ &= \frac{1}{N_m L_r L_\xi} K\left(\frac{r_i - r_i(\xi_l)}{h^r}, \frac{\xi - \xi_l}{h^\xi}\right), \end{aligned} \tag{36}$$

where K is a multivariate kernel density estimator, and L_r, L_ξ are the kernel supports along the r and ξ axes, respectively.

Using the law of total probability, $\hat{f}(r_i, \xi)$ can be found by calculating:

$$\hat{f}(r_i, \xi) = \tag{37}$$

$$= \sum_{l=0}^{N_m-1} \hat{f}(r_i, \xi \mid T[z_i(\xi_l)], T[z_1(\xi_l)]) p(T[z_i(\xi_l)], T[z_1(\xi_l)]).$$

We interpret the probability $p(T[z_i(\xi_l)], T[z_1(\xi_l)])$ as a measure of the correctness of calculating $a_i(\xi_l)$ using Eq. (32). If the noise is at least one order of magnitude smaller than the observed signals, the approximation of Eq. (32) holds. If the noise parameters can be estimated, for example in the case of normal distributed noise with a known variance σ^2, the probability of the noise being an order of magnitude smaller than the measurement $T[z_i(\xi_l)]$ or $T[z_1(\xi_l)]$, is:[5]

$$\begin{aligned} & p(T[z_i(\xi_l)], T[z_1(\xi_l)]) \equiv \\ & \equiv \min\{ \int_{-|l|}^{|l|} \frac{1}{\sigma\sqrt{20\pi}} e^{-\frac{v^2}{20\sigma^2}} dv, \ \int_{-|l|}^{|l|} \frac{1}{\sigma\sqrt{20\pi}} e^{-\frac{v^2}{20\sigma^2}} dv \}, \end{aligned} \tag{38}$$

where $l = T[z_i(\xi_l)]$.

[5]In the case where the noise parameters are unknown, we assume that $p(T[z_i(\xi_l)], T[z_1(\xi_l)])$ is constant.

We want to evaluate the conditional probability of $a_j(\xi)$, being represented by α_{i_k} parameters, given the ratio of the measurements $r_i(\xi_0 ... \xi_{(N_m-1)})$, i.e. Eq. (35). We can calculate this probability using a line integral over a scalar field, being the density $\hat{f}(r_i, \xi)$:

$$\begin{aligned} \mathbb{J}(\alpha_{i_k}) &\equiv p(\alpha_{i_k} \mid r_i(\xi_0 ... \xi_{(N_m-1)})) = \\ &= \int_{\xi_1}^{\xi_2} \hat{f}(a_i(\alpha_{i_k}; \xi), \xi) \sqrt{1 + [a_i'(\alpha_{i_k}; t)]^2} d\xi, \end{aligned} \tag{39}$$

where a_i' stands for the derivation with respect to ξ, and ξ_1, ξ_2 are the observation start and stop time/position instance, respectively.

The optimization can be executed by means of the Newton method, starting from several initial points as follows:

1) Take as an initial guess a vector of $\alpha_{i_k}^{(0)}$ parameters.
2) Use the vector $\alpha_{i_k}^{(m)}$ obtained from the previous step, and construct the gradient vector $\nabla \mathbb{J}(\alpha_{ij_k}^{(m)})$ and the Hessian matrix $Hess_{\mathbb{J}}(\alpha_{i_k}^{(m)})$, using:

$$\begin{aligned} \frac{\partial \mathbb{J}(\alpha_{i_k}^{(m)})}{\partial \alpha_{i_k}^{(m)}} &= \frac{\partial p(\alpha_{i_k}^{(m)} \mid r_i(\xi_0 ... \xi_{(N_m-1)}))}{\partial \alpha_{i_k}^{(m)}} \\ \frac{\partial^2 \mathbb{J}(\alpha_{i_k}^{(m)})}{\partial \alpha_{i_k}^{(m)} \partial \alpha_{i_j}^{(m)}} &= \frac{\partial^2 p(\alpha_{i_k}^{(m)} \mid r_i(\xi_0 ... \xi_{(N_m-1)}))}{\partial \alpha_{i_k}^{(m)} \partial \alpha_{i_p}^{(m)}}. \end{aligned} \tag{40}$$

3) Update the estimated parameters:

$$\alpha_{i_k}^{(m+1)} = \alpha_{i_k}^{(m)} - Hess_{\mathbb{J}}(\alpha_{i_k}^{(m)}) \nabla \mathbb{J}(\alpha_{i_k}^{(m)}). \tag{41}$$

4) Repeat steps 2 and 3 until convergence.

The initial points can be selected by using an approach similar to the application of the Hough transform in image processing [50].

A few implementation remarks are in order:

1) The integral of Eq. (39) should be found indefinitely. We, therefore, propose using the Epanechnikov radially symmetric kernel [51] which is defined as follows:

$$K(x, y) = \begin{cases} \frac{2}{\pi}(1 - x^2 - y^2) & (x^2 + y^2) \leq 1 \\ 0 & othewise \end{cases}. \tag{42}$$

2) If $a_i(\alpha_{i_k})$ renders the indefinite integral of Eq. (39) unsolvable, an approximation for $a_i(\alpha_{i_k})$ should be used.
3) It is usually preferable to define $g_i'(\xi) \equiv arctan(g_i(\xi))$ in order to eliminate the noise amplification accompanying the calculation of $T[z_i(\xi)]/T[z_1(\xi)]$. The definition of $r_i(\xi_l)$ to be inserted in Eq. (36) should be accordingly changed to $r_i(\xi_l) \equiv arctan(T[z_i(\xi_l)]/T[z_1(\xi_l)])$. After optimizing for the α_{i_k} parameters and finding $g_i'(\xi)$, $g_i(\xi)$ can be found using $g_i(\xi) = tan(g_i'(\xi))$.

C. Source Estimation

As we have already shown, the Zadeh's frequency response of the elements of the mixing matrix is independent of ω and, therefore, these elements belong to their centralizer. This means that the elements of the matrix are commutative, permitting the application of the matrix algebra mentioned in Corollary 9. As long as the determinant $a_1(\xi) - a_2(\xi) \neq 0$,[6] the system is invertible and Eq. (17) can be used to estimate the sources.

[6]In instances where $a_1(\xi) - a_2(\xi) \ll 1$ the system is singular or badly conditioned and the variational method should be used

D. A System for Generating Position Varying Instantaneous Image Mixtures

In the process of imaging through a semi-reflector, such as a plain glass window, the reflected image is superimposed on the transmitted one. The left optical setup shown in Fig. 3 depicts an optical system assembled in our lab for generating position varying instantaneous mixture of images. The glass is used as a mixer of transmitted and reflected obtained images. The position varying mixing is achieved by changing the lighting condition of the transmitted image, by using a non-uniform illumination. First mixture is acquired using room lighting whereas a second mixture is acquired using an extra non-uniform illumination.

E. Results

We tested our approach on simulated and real mixtures. For the simulated mixtures, two mixtures were obtained from two audio signals. The signals were sampled at a rate of 32K samples/sec, and mixed using time varying instantaneous filter matrix with the following coefficients:

$$g_{2j}(t) = \alpha_{2j_1} t^2 + \alpha_{2j_2} t + \alpha_{2j_3}. \tag{43}$$

The filters change the attenuation of the signals as a second degree polynomial function of time. Random noise with normal distribution was added to the mixtures, yielding a Peak-Mixture-to-Noise Ratio (PSNR) of 20 dB. The mixtures were 'sparsified' using STFT with window duration of $1/4$ of a second. For the parametric mixing system estimation, we estimated the probability density using the Epanechnikov radially symmetric kernel density estimation. The integral of Eq. (39) was indefinitely calculated and the intersections of the support of the kernel with the curve were found using Matlab solver. The optimization scheme was implemented using Matlab and the algorithm was initialized by several starting points and converged to two local maxima. The system was directly inverted by calculating the inverse of the mixing matrix, H^{-1}. Fig. 4 depicts the signals of mixtures of two voices. On the top left are the spectrograms obtained by using a STFT with a window duration of $1/4$ second. Shown on the top right are the separated estimated sources. On the top middle, we can see the kernel estimated probability density. The audio mixtures and separated sources can be found at www.visl.ac.il/ kaftory/...

The CSISR of the top examples of Fig. 4 increased from $4dB$ and $-4dB$, for the two mixed sources, to $28dB$ and $32dB$ after the separation.

The setup depicted in Fig. 3 was used for generating real mixtures. The mixtures were acquired with a Nikon D100 digital camera controlled by a computer. The PSNR for the noisiest mixture, which was estimated by taking consecutive identical pictures, was 40 dB. We define $g_i'(\xi) \equiv arctan(g_i(\xi))$ and assume that a second order polynomial is the estimated Taylor expansion of $g'i(\xi)$. Since images are not naturally sparse, we used the Haar wavelet packet for sparsification. The sparsest node (node 1,3) was chosen. Again, for the parametric mixing system estimation, we estimated the probability density using the Epanechnikov radially symmetric kernel density estimation. We initiated our algorithm with several starting parameters and the algorithm converged to two local maxima. The system was inverted directly by calculating the inverse of the mixing matrix, H^{-1}.

The bottom of Fig. 4 depicts results obtained in separation of reflection from a transmitted image. The mixtures were generated by the system shown on the left side of Fig. 3. The mixtures of the images are shown on the bottom left. One mixture was acquired under normal room-lighting condition and the other acquired with the addition of non-uniform lighting to the transmitted image. The estimated separated sources are shown in the bottom right. The Mutual Information of the mixtures is 0.3 and 0.15 for the separated sources. The kernel-estimated probability density, obtained by selecting pixels corresponding to wavelet packet coefficients exceeding the threshold, is shown on the middle.

VI. Blind Separation of Time/Position Varying Single-path Mixtures

Here[7], we assume that the mixing filters have the form of Eq. (6), where there is no attenuation. In this section, we use as an example, two mixtures of a transmitted image and a phantom reflected from

[7]Some of the methods and the results of this section where published in [52], [53]

a curved semi-reflector, acquired from slightly different locations. When the semi-reflector is not flat, as is the case in a front windshield of a car or the canopy of a cockpit, the reflected image is usually distorted. Furthermore, the distortion of the reflection varies as a function of the viewing position [54]. We model these image mixtures in the context of a position varying single-path BSS problem. To this end, we following:

I. The model of the single-path mixing coefficient is arbitrary, but is a smooth function.
II. The dependency of the reflection and the transmission coefficients on the viewing angle is negligible. Therefore, the image intensity does not change when the camera position varies.
III. The image sources contain edges or other features.

Considering two different mixtures and representing them in matrix form, the BSS problem can be written explicitly as:

$$\begin{bmatrix} z_{\lambda_1} \\ z_{\lambda_2} \end{bmatrix} = \begin{bmatrix} h_{R_1} & h_{D_1} \\ h_{R_2} & h_{D_2} \end{bmatrix} \star \begin{bmatrix} R_\lambda \\ D_\lambda \end{bmatrix} + \eta. \tag{44}$$

, where z_{λ_1} and z_{λ_2} are the mixtures observed from two different camera positions. h_R and h_D, defined by:

$$h_R(\underline{\xi}, \underline{\xi}') \equiv \delta\left(\underline{\xi}' - M_R(\underline{\xi})\right), \quad h_D(\underline{\xi}, \underline{\xi}') \equiv \delta\left(\underline{\xi}' - M_D(\underline{\xi})\right), \tag{45}$$

where M_R and M_D are mapping between the reflected image coordinate system and the transmitted image coordinate system to the camera system respectively [52]. We explicitly define the filters g_i of Eq. 12 as:

$$h_{R_2} = g_R \star h_{R_1}, \quad h_{D_2} = g_D \star h_{D_1}. \tag{46}$$

Solving for g_R and g_D yields:

$$g_R = \delta\left(\underline{\xi}' - M_{R_2}(\underline{\xi}) + M_{R_1}(\underline{\xi})\right), \tag{47}$$

and

$$g_D = \delta\left(\underline{\xi}' - R_{D_2}(\underline{\xi}) + M_{D_1}(\underline{\xi})\right). \tag{48}$$

A. Sparsification using Scale Invariant Feature Transform

The Zadeh transform of one of the elements of the mixing matrix is:

$$\begin{aligned} &\mathcal{H}_{Z_R}(\underline{\xi}, \underline{\omega}) = \\ &\int_{-\infty}^{\infty} \delta\left(\underline{\xi}' - M_R(\underline{\xi})\right) e^{j\left(\underline{\omega}(\underline{\xi}-\underline{\xi}')^T\right)} d\underline{\xi} = \\ &= e^{j\left(\underline{\omega}(\underline{\xi}-M_R(\underline{\xi}))\right)}. \end{aligned} \tag{49}$$

Since it is a function of both $\underline{\omega}$, and $\underline{\xi}$, finding its centralizer is a challenging task. None of the common sparsification transformations, which can be accounted for by conventional filters, belongs to the centralizer and is invariant to the mixing system. The zero order Taylor approximation of the mixing filters, calculated around some point is a translation of that point. The first order scales the image about this point. The second and higher order, produce nonlinear stretching to this image point. Therefore, the mixing filters can be approximated by local affine transforms. The Scale Invariant Feature Transform (SIFT) [55], which cannot be accounted for by a filter, but is invariant to local affine transforms, can be used as a sparsification transformation invariant to the mixing filters. SIFT transforms an image into a large collection of local feature vectors, based on the appearance of an object of special interest (key) points. Each feature vector is translation, rotation and scale invariant as well as invariant, to illumination changes and 3D projection. The feature vectors are highly distinctive and can, therefore, be regarded as a sparse representation, where only a small percentage of the pixels are chosen.

B. Mixing Matrix Estimation

Suppose we observe in one of the mixtures, in some position $\underline{\xi}_0$, the existence of a matching keypoint to the other mixture in the position $\underline{\xi}_1$, and the keypoint belongs to the transmitted image. $M_{D_1}(\underline{\xi})-M_{D_2}(\underline{\xi})$ is the difference (measured in pixels) between the mapping of a point in the transmitted image to the first and second observed images. Therefore, for the matching keypoints this value is $M^1_{D_1}(\underline{\xi}) - M_{D_1}(\underline{\xi}) = \underline{\xi}_0 - \underline{\xi}_1$. Recalling Eq. (48), the value of $g_D(\underline{\xi})$ is known for this keypoint. For matching keypoints which belong to the reflected image, the value of g_R is known. Therefore, by scatter-plotting the location difference of the matching keypoints, two surfaces can be estimated. One corresponds to g_D and the other to g_R. We can usually assume that the transmitted image is not distorted but may be slightly shifted between the mixtures, and solve the problem of grouping the keypoints to g_R or g_D. It is done by first grouping all the matching keypoints of which their relative offsets are consistent with a small, close to zero shift, and assigning them to the surfaces of g_D. The remaining keypoints are assigned to g_R and used in estimating the surface of g_R by utilizing a surface fitting technique. If we have a-priori information about the curvature of the semi-reflector, we can assume a parametric surface fitting model for the surface estimation. Otherwise, we can assume that the surface is smooth and apply a non-parametric surface fitting with smoothing constraints.

C. Variational Source Estimation

From the Zadeh's transform of the mixing filters in Eq. (49) one may conclude that the elements of the mixing matrix do not commute. Therefore, a direct inversion of the mixing system is not feasible. We implement a variational framework for solving the problem. Recalling the BSS problem,

$$\begin{aligned} z_{\lambda_1} &= R'_\lambda + D'_\lambda + \eta_1, \\ z_{\lambda_2} &= g_R \star R'_\lambda + g_D \star D'_\lambda + \eta_2, \end{aligned} \tag{50}$$

we filter both sides of the first equation with the position varying filter g_R and subtract it from the second equation. This yields the following equation, to be solved for D'_λ:

$$z_{\lambda_2} - g_R \star z_{\lambda_1} = (g_D - g_R) \star D'_\lambda + \eta, \tag{51}$$

where we used the distributivity property of $\star$.

A variational approach to solving Eq. (51) is by minimizing the cost functional:

$$\mathbb{J} = \| \, z_{\lambda_2} - g_R \star z_{\lambda_1} - (g_D - g_R) \star D'_\lambda \, \|^2 + w\mathbf{R}(D'). \tag{52}$$

The regularization operator, $\mathbf{R}(D')$, that we use for color images, is based on the Beltrami flow. Sochen et al.,. [56], interpret an image as a manifold (surface) embedded in a high dimensional space, where x, and y are two spatial coordinates of this space, and the intensity at each of the λ channels is represented as an additional dimension. Hence, a color image, such as the reflected or the transmitted image, is a manifold embedded in a 5-dimensional space. From this viewpoint, image regularization can be interpreted as a process that minimizes the surface area of this manifold. The surface area of an image is measured by the Polyakov action [57]. It is given for the transmitted image by:

$$\mathbf{R}(D') = \iint_\Omega \sqrt{\det(\mathbf{G}_{\mathtt{D}})} dx dy, \tag{53}$$

where $\mathbf{G}_{\mathtt{D}}$ is a 2×2 matrix. Each of the matrix entries, depends on the spatial location. Their values are given [58] by

$$\begin{aligned} \mathbf{g}^{\mathtt{D}}_{11} &= 1 + \rho^2 \textstyle\sum_\lambda (\partial D'_\lambda / \partial x)^2 \\ \mathbf{g}^{\mathtt{D}}_{12} = \mathbf{g}^{\mathtt{D}}_{21} &= \rho^2 \textstyle\sum_\lambda \dfrac{\partial D'_\lambda}{\partial x} \dfrac{\partial D'_\lambda}{\partial y} \\ \mathbf{g}^{\mathtt{D}}_{22} &= 1 + \rho^2 \textstyle\sum_\lambda (\partial D'_\lambda / \partial y)^2 \ , \end{aligned} \tag{54}$$

where ρ is a parameter for scaling the intensity dimensions. It is useful not to use the Polyakov action, but to use a modified version (by multiplying it by a positive function) where its derivative is the Beltrami flow which is defined as:

$$Beltrami \equiv \frac{1}{\sqrt{\det(\mathbf{G}_{\mathtt{D}})}}\mathcal{D}iv\left[\sqrt{\det(\mathbf{G}_{\mathtt{D}})}(\mathbf{G}_{\mathtt{D}})^{-1}\nabla D'_{\lambda}\right]. \tag{55}$$

The properties of using the Beltrami flow for the restoration of color images are investigated thoroughly in [59] and [60]. Some of these properties are:

1) Forcing the color channels to spatially align and therefore to suppress color distortions.
2) Reducing the noise.
3) Preserving the image edges.

Minimizing $\mathbb{J}$, [56], accomplished by reaching $d\mathbb{J}/dD'_{\lambda} = 0$ or, equivalently, solving its Euler-Lagrange equation:

$$\begin{aligned}&\textstyle\sum_{\lambda}(g_D - g_R)^T \star (z_{\lambda_2} - g_R \star z_{\lambda_1} - (g_D - g_R) \star D'_{\lambda})\\ &\quad + \frac{w}{\sqrt{\det(\mathbf{G}_{\mathtt{D}})}}\mathcal{D}iv\left[\sqrt{\det(\mathbf{G}_{\mathtt{D}})}(\mathbf{G}_{\mathtt{D}})^{-1}\nabla D'_{\lambda}\right] = 0,\end{aligned} \tag{56}$$

where $(g_D - g_R)^T$ is the position varying filter obtained by switching the place along the coordinates $\underline{\xi}$ and $\underline{\xi}'$, ∇D_{λ} is the spatial gradient of D'_{λ} and $\mathcal{D}iv$ is the divergence operator. Eq. (56) is a nonlinear partial differential equation (PDE). Rather than solving it directly, we use the Fixed Point Lagged Diffusive method, used in [61]. By means of this method, the PDE can be solved by lagging the nonlinear term of the Beltrami operator one iteration behind. Then, for example, by knowing ${D'}_{\lambda}^{(t)}$ in some iteration t , ${D'}_{\lambda}^{(t+1)}$ can be found by solving a linear PDE, while applying a conjugate gradient minimization scheme.

In operator form, we obtain the following operator definitions:

$$\begin{aligned}\mathcal{L}({D'}_{\lambda}^{(t)}){D'}_{\lambda}^{(t+1)} &\equiv (g_D - g_R)^T \star (g_D - g_R) \star {D'}_{\lambda}^{(t+1)} - \\ &- \frac{\gamma}{\sqrt{\det(\mathbf{G}_{\mathtt{D}^{(t)}})}}\mathcal{D}iv\left[\sqrt{\det(\mathbf{G}_{\mathtt{D}^{(t)}})}(\mathbf{G}_{\mathtt{D}^{(t)}})^{-1}\nabla {D'}_{\lambda}^{(t+1)}\right],\end{aligned} \tag{57}$$

and

$$\mathcal{K} \equiv (g_D - g_R)^T \star (z_{\lambda_2} - g_R \star z_{\lambda_1}). \tag{58}$$

Eq. (56) can be written using the above operator definition as:

$$\mathcal{L}({D'}_{\lambda}^{(t)}){D'}_{\lambda}^{(t+1)} - \mathcal{K} = 0. \tag{59}$$

A direct solution of these equations, as required by each minimization step, would be:

$${D'}_{\lambda}^{(t+1)} = \mathcal{L}({D'}_{\lambda}^{(t)})^{-1}\mathcal{K}. \tag{60}$$

Since it is difficult to find and invert $\mathcal{L}({D'}_{\lambda}^{(t)})^{-1}$, the step $d{D'}_{\lambda}^{(t)}$ is introduced:

$${D'}_{\lambda}^{(t+1)} = {D'}_{\lambda}^{(t)} + d{D'}_{\lambda}^{(t)}. \tag{61}$$

The step $d{D'}_{\lambda}^{(t)}$ can be found by solving:

$$\mathcal{L}({D'}_{\lambda}^{(t)})d{D'}_{\lambda}^{(t)} = \mathcal{K} - \mathcal{L}({D'}_{\lambda}^{(t)}){D'}_{\lambda}^{(t)}. \tag{62}$$

Eq. (62) can be solved by using the conjugate gradient method.

A similar restoration process with the Beltrami operator, was used in [62] for the unmixing and restoration of color images taken through a scattering medium.

D. System for Generating Position Varying Single-path Mixtures

Optical systems which yield position varying image mixtures are depicted in Fig. 3. Shown on the right-hand side is a curved semi-reflector used as a mixer between a transmitted image and a reflection. The position-varying single-path mixing is imposed the curvature of the semi-reflector. Two different mixtures are acquired by moving the camera to slightly different positions, which results in approximately the same transmitted image, but different distortions of the reflected image.

E. Results

We tested our approach on simulated and real mixtures. For the simulation, we implemented a simulator based on ray-tracing and used it to simulate a superposition of a reflected and transmitted image. Two observation points were used to obtain two slightly different mixtures. The shape of the semi-reflector was chosen to be a sphere, thus, producing a reflection with a fisheye-lens effect. We also assumed that the semi-reflector is very thin, to avoid distortions of the transmitted image. Finally, Gaussian noise was added to the mixtures, yielding a peak-mixture-to-noise ratio of 25 dB. For the real mixtures, the setup depicted in Fig. 3 was used. Instead of a semi-reflector made out of glass, we curved a thin polycarbonate sheet. The mixtures were acquired with a Nikon D100 digital camera interfaced with a computer. The PSNR for the noisiest mixture, which was estimated by taking consecutive identical pictures, was 40 dB.

The mixtures were sparsified using SIFT.[8] Following the keypoint matching we use the parametric surface fitting on the simulated mixtures and a nonparametric on the experiments , by first calculating the location difference of corresponding SIFT keypoints. We take advantage of the fact that the transmitted image is not distorted. Thus, the location difference between the corresponding SIFT keypoints is constant. We estimate this constant by finding the maximum of the histogram of the location differences. After removing all the features corresponding to this constant, a second degree polynomial surface fitting is applied to the rest.

Fig. 5 depicts the results. The mixtures of the images are shown on the left. The estimated surfaces obtained by the parametric surface fitting are shown in the middle. The separated, estimated, sources are shown on the right. The estimated sources are well separated.

The Mutual Information of the images, which was 2.7 and 1.3 for the mixtures in the simulation and the experiment respectively, was reduced to 0.8 and 0.6, respectively, after the separation.

VII. Blind Separation of Time varying Multi-path Mixtures

We limit ourselves to mixing filters which are time-varying, attenuated-and-delayed, versions of fixed channel distortions:

$$h_{ij}(t,\tau) = a_{ij}(t) f_{ij}(d_{ij}(t) - \tau), \tag{63}$$

where a_{ij} is a time-varying attenuation, f_{ij} is a Finite Impulse Response filter and d_{ij} is a time-varying delay function. In this section, we assume the following:

I. Apart from some instances, the zero order Taylor approximation of the Zadeh transform of the multi-path mixing coefficients, around some instances confined to a small window, is sufficient to represent the function in that window.

II. The sources are either sparse in their native domain, or can be sparsely represented in the time-frequency domain.

We assume that these mixing filters have finite support, with a maximum support of size $2L_M$. We can, therefore, find a window of size $2L_T$, $L_T \gg L_M$, around the time instance t, in which $h_{ij}(t, \tau < t - L_T) = 0$ and $h_{ij}(t, \tau > t + L_T) = 0$. Consequently, we can state that:

$$h_{ij}(t,\tau) = h_{ij}(t,\tau) wind(t - \tau), \tag{64}$$

[8] SIFT Matlab code can be downloaded from www.cs.ubc.ca/lowe/keypoints

where $wind(t-\tau)$ denotes a unit window function centered at $\tau = t$ with support of $2L_T$.

The BSS problem can be written as:

$$z_i(t) = \sum_j \int_{-\infty}^{\infty} h_{ij}(t,\tau) wind(t-\tau) s_j(\tau) d\tau + \eta =$$

$$= \sum_j \int_{-\infty}^{\infty} h_{ij}(t,\tau) s_j(t,\tau) d\tau + \eta, \tag{65}$$

where we define $s(t,\tau) \equiv wind(t-\tau)s(\tau)$. We note that $s(t)$ can be calculated by $s(t) = \int_{-\infty}^{\infty} \delta(t-\tau)s(t,\tau)d\tau$.

Using Zadeh's frequency response, Eq. (65) can be written as:

$$z_i(t) = \frac{1}{2\pi} \sum_j \int_{-\infty}^{\infty} \mathcal{H}_{Z_{ij}}(t,\omega) \mathcal{S}_{F_j}(t,\omega) e^{j\omega t} d\omega, \tag{66}$$

where $\mathcal{H}_{Z_{ij}}(t,\omega)$ is the Zadeh frequency response of h_{ij}, and $\mathcal{S}_{F_j}(t,\omega)$ is the Fourier transform of $s_j(t,\tau)$ along the τ axis.

The BSS problem can be written in the Zadeh time-frequency domain as:

$$\mathcal{Z}_{Z_i}(t,\omega) = \sum_j \mathcal{H}_{Z_{ij}}(t,\omega) \mathcal{S}_{F_j}(t,\omega) + \tilde{\eta}, \tag{67}$$

where $\tilde{\eta}$ is the time-frequency representation of the Gaussian noise, assumed to be constant. We can regard $\mathcal{Z}_{Z_i}(t,\omega)$ as the frequency representation of the output of the mixing system given an input at the instance t using the filters $h_{ij}(t,\tau)$, with the addition of some noise constant. Clearly, in a similar way to Eq. (66), $z_i(t)$ can be found using the inverse Zadeh transform of $\mathcal{Z}Z_i(t,\omega)$:

$$z_i(t) = \frac{1}{2\pi} \int_{-\infty}^{\infty} \mathcal{Z}_{Z_i}(t,\omega) e^{j\omega t} d\omega. \tag{68}$$

The modified BSS problem can be written in the Zadeh domain as:

$$\mathcal{Z}_{Z_i}(t,\omega) = \sum_j \mathcal{G}_{Z_{ij}}(t,\omega) \mathcal{S}'_{F_j}(t,\omega) + \tilde{\eta}, \tag{69}$$

where $\mathcal{G}_{Z_{ij}}(t,\omega) = \mathcal{H}_{Z_{ij}}(t,\omega)\mathcal{H}^{-1}_{Z_{1j}}(t,\omega)$ and $\mathcal{S}'_{F_j}(t,\omega) = \mathcal{H}_{Z_{1j}}(t,\omega)\mathcal{S}_{F_j}(t,\omega)$, where a method for finding the sources $s'_1(t)$ and $s'_2(t)$ out of $\{S'_{F_1}(t,\omega)$ and $\mathcal{S}'_{F_2}(t,\omega)$ is by calculating:

$$s'(t) = \int_{-\infty}^{\infty} \mathcal{S}'_F(t,\omega) e^{j\omega t} d\omega.$$

A. Sparsification Using Short Time Fourier Transform

As stated earlier, $\mathcal{Z}_{Z_i}(t,\omega)$ is the time-frequency representation of the mixtures in the Zadeh transform domain. In a similar way to the Short Time Fourier Transform (STFT), and as one of the assumptions mentioned in the introduction, $\mathcal{Z}_{Z_i}(t,\omega)$ is a sparse representation of audio and other harmonic signals.

Utilizing the assumption stated in the introduction, we can find some windows of size $2L_L$, over which the zero order Taylor approximation is sufficient to represent the Zadeh transform of the mixing filters in these windows. We set the size of L_T such that $L_L > L_T + L_M$, where $2L_T$ is the size of the window used for calculating $s_j(t,\tau)$, and $2L_M$ is the maximum support of the mixing filters.

It is shown in [41] that if the frequency content of the sources does not change over the same window where the zero order Taylor approximation is sufficient to represent the Zadeh transform of the mixing filters, the STFT with windows of size $2L_L$ of the observed mixtures $z_i(t)$, provides an estimation to $\mathcal{Z}_Z(t,\omega)$.

Since this estimation is sparse, the STFT under the assumptions can be regarded as a sparsification transformation.

B. Mixing Matrix Estimation

Sparse signals represented in the time-frequency space enable the estimation of the mixing system, since there are many frequencies and time instances, over which only one source is active. Therefore, $\mathcal{G}_{ij}(t,\omega)$ can be found from:

$$\mathcal{G}_{Z_{ij}}(t,\omega) \approx \mathcal{Z}_{Z_i}(t,\omega)\mathcal{Z}_{Z_1}(t,\omega)^{-1}. \tag{70}$$

The Zadeh frequency responses of filters of the type used in this section, are:

$$\mathcal{H}_{Z_{ij}}(t,\omega) = a_{ij}(t)\mathcal{F}_{F_{ij}}(\omega)e^{-j\omega(t-d_{ij}(t))}, \tag{71}$$

where $\mathcal{F}_{F_{ij}}(\omega)$ is the Fourier transform of the fixed filter $f_{ij}(t-\tau)$.

The value of the mixing filter $\mathcal{G}_{ij}(t,\omega)$ is therefore:

$$\mathcal{G}_{Z_{ij}}(t,\omega) = \frac{a_{ij}(t)F_{F_{ij}}(\omega)e^{-j\omega(t-d_{ij}(t))}}{a_{1j}(t)F_{F_{1j}}(\omega)e^{-j\omega(t-d_{1j}(t))}}. \tag{72}$$

The filter $\mathcal{G}_{Z_{ij}}(t,\omega)$ is a complex function. Therefore, instead of finding it directly, we estimate its amplitude and phase separately.

We define the angle $\psi_i(t,\omega)$ as follows:

$$\psi_i(t,\omega) = \tan^{-1}\left(\frac{|\mathcal{Z}_{Z_i}(t,\omega)|}{|\mathcal{Z}_{Z_1}(t,\omega)|}\right). \tag{73}$$

According to the assumptions related to properties of sources that are sparse in their time-frequency domain representation, there are time instances t_n and frequencies ω_m where only one source is active. We scatter-plot the points $\psi_1(t_n,\omega_m)$ and $\psi_2(t_n,\omega_m)$ for some fixed ω as a function of t. The points lie on one of the curves $\tilde{\psi}_{1j}(t,\omega)$ or $\tilde{\psi}_{2j}(t,\omega)$, where $\tilde{\psi}_{ij}(t,\omega)$ is defined as follows:

$$\tilde{\psi}_{ij}(t,\omega) = \tan^{-1}\left(\frac{a_{ij}(t)\left|\mathcal{F}_{F_{ij}}(\omega)\right|}{a_{1j}(t)\left|\mathcal{F}_{F_{1j}}(\omega)\right|}\right). \tag{74}$$

Note that the above curve is continuous, since $\tilde{\psi}_{ij}(t,\omega)$ does not depend on the value of the source j. Therefore, if we assume that $a_{ij}(t)$ is a continuous functions of t, $\tilde{\psi}_{ij}(t,\omega)$ is also a continuous function of t, bounded between 0 and $\pi/2$. We should note that we use the inverse tangent of the ratio $a_{ij}(t)\left|F_{F_{ij}}(\omega)\right|/a_{1j}(t)\left|F_{F_{1j}}(\omega)\right|$ in order to suppress the amplification of the noise in the cases where the denominator is close to zero.

We define the phase shift $\Delta\phi_i(t,\omega)$ as follows:

$$\Delta\phi_i(t,\omega) = \angle\mathcal{Z}_{Z_i}(t,\omega) - \angle\mathcal{Z}_{Z_1}(t,\omega), \tag{75}$$

where the symbol $\angle$ denotes the phase.

We scatter-plot the points $\Delta\phi_1(t_n,\omega_m)$ and $\Delta\phi_2(t_n,\omega_m)$ on a graph for some fixed ω as a function of t. The points lie on one of the curves $\Delta\tilde{\phi}_{1j}(t,\omega)$ and $\Delta\tilde{\phi}_{2j}(t,\omega)$, where $\Delta\tilde{\phi}_{ij}(t,\omega)$ is defined as follows:

$$\Delta\tilde{\phi}_{ij}(t,\omega) = \angle\mathcal{F}_{F_{ij}}(\omega) - \angle\mathcal{F}_{F1j}(\omega) + \omega(d_{ij}(t) - d_{1j}(t))). \tag{76}$$

In this case too, the above curve is continuous, since $\Delta\tilde{\phi}_{ij}(t,\omega)$ does not depend on the value of the source j. Therefore, if we assume that $d_{ij}(t)$ is a continuous function of t, $\Delta\tilde{\phi}_{ij}(t,\omega)$ is also a continuous function of t, bounded between 0 and 2π with a 2π fold.

It is observed that the values of the mixing filters $\mathcal{G}_{Z_{ij}}$ can be found by:

$$\mathcal{G}_{Z_{ij}}(t,\omega) = tan\left(\tilde{\psi}_{ij}(t,\omega)\right) e^{j\Delta\tilde{\phi}_{ij}(t,\omega)}. \tag{77}$$

The objective is, therefore, to find the curves out of the cluttered points. This can be done either by using a parametric estimation, or a non-parametric estimation using methods described in the previous sections.

C. Source Estimation

In the time-frequency domain, the filters $\mathcal{G}_{Z_{ij}}(t,\omega)$ of the above form, are commutative. Therefore, a direct inversion of the problem is feasible. In cases where $\mathcal{G}_{Z_{22}}(t,\omega) - \mathcal{G}_{Z_{21}}(t,\omega) \ll 1$ the system is singular or badly conditioned. A variational methods should then be used. Two variational methods – one in the combined time-frequency domain and the other in the time domain are presented in [41].

D. Results

We tested our approach on simulated audio signals in a semi-realistic acoustic scenario, in which a reporter is speaking to a 2-microphone array, while an emergency vehicle is passing nearby. The functions $a_{ij}(t)$ and $d_{ij}(t)$ are calculated for this scenario as:

$$a_{ij}(t) = \frac{1}{q_{ij}(t)}, \qquad d_{ij}(t) = t - \frac{q_{ij}(t)}{c}, \tag{78}$$

where c is the speed of sound and q_{ij} is the distance between the j^{th} source to the i^{th} sensor.

The signals recorded from the reporter and the emergency vehicle were sampled with anti-aliasing filter at the rate of $4K$ samples /second. We assumed that the microphones were close to each other, therefore the time invariant atmospheric transfer function obeys $f_{11} = f_{21}$ and $f_{12} = f_{22}$. Finally, Gaussian noise was added to the mixtures, yielding a mixture-to-noise ratio of 20 dB. The value of $Z_i(t,\omega)$ was obtained using a windowed Fourier transform with a window of length 400 samples.

We scatter-plot the points $\psi(t_n,\omega_m)$ for the time and frequencies, where the absolute values of the windowed Fourier transform of the mixtures are above the threshold. It is done for each ω as a function of t. Since according to the assumptions, this ratio should be the same for all ω, we take the maximum of the histogram and plot it as a function of time. We use the parametric curve fitting assuming a polynomial of various degrees, until a good approximation to the curves $\tilde{\psi}_{ij}(t,\omega)$ is achieved. We then scatter-plot the points $\Delta\phi(t_n,\omega_m)/\omega_m$ for the time and frequencies where the absolute values of the windowed Fourier transform of the mixtures are above the threshold. These points are independent of ω. We use the parametric curve fitting, assuming a polynomial of various degrees, until a good approximation to the curves $\Delta\tilde{\psi}_{ij}(t,\omega)/\omega$ is achieved.

Fig. 6 depicts the results. The estimation of $\tilde{\psi}_{ij}(t,\omega)$ and $\Delta\tilde{\phi}_{ij}(t,\omega)/\omega$ using a polynomial fit are shown on the right. We use $\tilde{\psi}_{ij}(t,\omega)$ and $\Delta\tilde{\phi}_{ij}(t,\omega)$ to construct $\mathcal{G}_{Z_{ij}}(t,\omega)$ by:

$$\mathcal{G}_{Z_{ij}}(t,\omega) = tan\left(\tilde{\psi}_{ij}(t,\omega)\right) e^{j\Delta\tilde{\phi}_{ij}(t,\omega)}. \tag{79}$$

The system is inverted using the variational approach in the time-frequency domain. The spectrogram of the mixtures is depicted on the left of Fig. 6 whereas the estimation of $\tilde{\psi}_{ij}(t,\omega)$ and $\Delta\tilde{\psi}_{ij}(t,\omega)/\omega$ are depicted in the middle and the estimated sources are depicted on the right. The mutual information of 1.6 of the mixtures, was reduced significantly to 0.7 for the separated sources.

VIII. Conclusions

Previous studies stated that the separation of time/position varying mixing system can be achieved by using an online algorithm of instantaneous or convolutive BSS. However, since all of the methods for the instantaneous and convolutive BSS, find an inverse to the mixing system using matrix algebra, they are applicable to time/position varying mixtures only under the assumption that the zero order Taylor approximation of the filters estimates the mixing system, and that the inverse system is not badly conditioned. In our study of time/position varying systems, we proved that in the general case the mixing filters do not commute and therefore inversion of the mixing system using matrix algebra is not feasible. We further found in the Zadeh time-frequency domain the conditions under which filters are commutative and consequently, an inverse filter exists. Thus, in most cases, an online form of existing instantaneous or convolutive BSS techniques does not solve the time/position varying BSS problem.

Instead of using an online form of instantaneous or convolutive BSS, we use the SSCA approach in a batch processing manner. We study the conditions which allow the application of the SSCA, and show that using an appropriate sparsification operator enables the estimation of the mixing system, as long as a proper threshold is imposed, so that the above-threshold instances are frequent enough and have a good signal-to-noise ratio. Estimation of the mixing system enables the system inversion which can be done directly by matrix inversion. For cases where matrix algebra cannot be used to invert the system, or where the inverse system is badly conditioned, we developed a variational approach for solving the inverse problem.

The demonstration of our SSCA approach along with the methods for sparsification and parametric and non-parametric mixing matrix estimation shows the feasibility of using the SSCA for the solution of various time/position varying BSS problems. This was demonstrated on simulated and experimental data, obtained from three types of mixtures representing many real-life applications.

Appendix

Proof of Proposition 1

The proof is only roughly outlined. The detailed proof can be found in [41]. By the definition of the conditional probability, and assuming that the variables are independent, we get:

$$p\left(CSISR > th_1, CSNR > th_2 \mid z_i = z_i(\underline{\xi}_0)\right) = \\ = \frac{p(CSISR > th_1 \cap z_i = z_i(\underline{\xi}_0))}{p(z_i = z_i(\underline{\xi}_0))} \cdot \\ \cdot \frac{p(CSNR > th_2 \cap z_i = z_i(\underline{\xi}_0))}{p(z_i = z_i(\underline{\xi}_0))}. \tag{80}$$

Starting with the denominator, z_i is a random variable which equals the sum of three independent random variables: $h_{i1} \star s_1$, $h_{i2} \star s_2$ and η_i. The PDF of z_i is therefore given by convolving the PDF of the random variables. For the numerator, we find the intersection of $CSISR > th_1$ and $h_{i1} \star s_1 + h_{i2} \star s_2 = z_i(\underline{\xi}_0)$, and the intersection of $CSNR > th_2$ and $h_{i1} \star s_1 + h_{i2} \star s_2 = z_i(\underline{\xi}_0)$.

Proof of Proposition 3

Using the inverse fourier transform of $S_F(\underline{\omega})$:

$$s(\underline{\xi}) = \frac{1}{2\pi} \int_{-\infty}^{\infty} S_F(\underline{\omega}) e^{j\underline{\omega}\underline{\xi}^T} d\underline{\omega}, \tag{81}$$

the system can be written as:

$$z(\underline{\xi}) = \int_{-\infty}^{\infty} h(\underline{\xi}, \underline{\xi}') \frac{1}{2\pi} \int_{-\infty}^{\infty} S_F(\underline{\omega}) e^{j\underline{\omega}\underline{\xi}'^T} d\underline{\omega} d\underline{\xi}'. \tag{82}$$

Changing the order of integration yields:

$$z(\underline{\xi}) = \frac{1}{2\pi} \int_{-\infty}^{\infty} S_F(\underline{\omega}) \left(\int_{-\infty}^{\infty} h(\underline{\xi}, \underline{\xi}') e^{j\underline{\omega}\underline{\xi}'^T} d\underline{\xi}' \right) d\underline{\omega}, \tag{83}$$

which is equal to:

$$z(\underline{\xi}) = \frac{1}{2\pi} \int_{-\infty}^{\infty} S_F(\underline{\omega}) \left(\int_{-\infty}^{\infty} h(\underline{\xi}, \underline{\xi}') e^{-j\underline{\omega}(\underline{\xi}-\underline{\xi}')^T} e^{j\underline{\omega}\underline{\xi}^T} d\underline{\xi}' \right) d\underline{\omega}$$

$$= \frac{1}{2\pi} \int_{-\infty}^{\infty} S_F(\underline{\omega}) H_Z(\underline{\xi}, \underline{\omega}) e^{j\underline{\omega}\underline{\xi}^T} d\underline{\omega}, \tag{84}$$

where we used the definition of the Zadeh transform.

Proof of Theorem 5

By the definition of an inverse filter:

$$\int_{-\infty}^{\infty} g(\underline{\xi}, \underline{\xi}'') h(\underline{\xi}'', \underline{\xi}') = \delta(\underline{\xi} - \underline{\xi}') = \boldsymbol{1}. \tag{85}$$

Taking the Zadeh transform of both sides, and using Lemma 4, we get:

$$\begin{aligned} &\sum_{r=0}^{n} \frac{\partial^r G_Z(\underline{\xi}, \underline{\omega})}{\partial (j\underline{\omega})^r} \frac{\partial^r H_Z(\underline{\xi}, \underline{\omega})}{\partial \underline{\xi}^r} = \\ &= \int_{-\infty}^{\infty} \delta(\underline{\xi} - \underline{\xi}') e^{-j\underline{\omega}(\underline{\xi}-\underline{\xi}')^T} d\underline{\xi}' = 1. \end{aligned} \tag{86}$$

Proof of Proposition 6

We prove it by an example. Consider the time varying filter which down-scales the axis by a factor of two, $h(\underline{\xi}, \underline{\xi}') = \delta(2\underline{\xi} - \underline{\xi}')$, and the delay filter which delays the signal by one unit is $g(\underline{\xi}, \underline{\xi}') = \delta(\underline{\xi} - 1 - \underline{\xi}')$. Clearly, if scaling precedes delaying, the scaled signal is delayed by one unit. If delaying precedes scaling, the scaled signal is only delayed by half a unit:

$$\begin{aligned} g \star h &= \int_{-\infty}^{\infty} \delta(\underline{\xi} - 1 - \underline{\xi}'') \delta(2\underline{\xi}'' - \underline{\xi}') d\underline{\xi}'' = \\ &= \delta(2\underline{\xi} - 2 - \underline{\xi}') \neq \\ h \star g &= \int_{-\infty}^{\infty} \delta(2\underline{\xi} - \underline{\xi}'') \delta(\underline{\xi}'' - 1 - \underline{\xi}') d\underline{\xi}'' = \\ &= \delta(2\underline{\xi} - 1 - \underline{\xi}'). \end{aligned} \tag{87}$$

Proof of Theorem 8

We have to show that the set is a commutative group over addition and a monoid over the operator $\star$. The first part is trivial, since 2n-dimensional time/position varying filters contain the set of real numbers $\mathbb{R}^{2n}$, which is a commutative group over addition. In order to prove that the set is a monoid over the operator, $\star$, we have to prove that it is a semigroup with the identity element. This means that it is a closed set under $\star$, has the associativity property and includes an identity element. An inverse is not required. By definition, the operation $\star$ with the set of time/position varying filters is a closed set ($\star : \mathbb{R}^{2n} \star \mathbb{R}^{2n} \rightarrow \mathbb{R}^{2n}$). The associativity can be proven by:

$$f \star (g \star h) = \int_{-\infty}^{\infty} f(\underline{\xi}, \underline{\xi''}) \left(\int_{-\infty}^{\infty} g(\underline{\xi''}, \underline{\xi'''}) h(\underline{\xi'''}, \underline{\xi'}) d\underline{\xi'''} \right) d\underline{\xi''}. \tag{88}$$

Changing the order of integration results in the following:

$$\int_{-\infty}^{\infty} \left(\int_{-\infty}^{\infty} f(\underline{\xi}, \underline{\xi''}) g(\underline{\xi''}, \underline{\xi'''}) d\underline{\xi''} \right) h(\underline{\xi'''}, \underline{\xi'}) d\underline{\xi'''} = (f \star g) \star h. \tag{89}$$

and the identity element which was defined by $\boldsymbol{1} \equiv \delta(\underline{\xi} - \underline{\xi'})$, is an identity element of the operator $\star$ and the set of 2n-dimensional time/position varying filters. The non-commutativity property was proven in Proposition 6.

*

Acknowledgment Research supported in part by the Ollendorff Center for Vision and Image Sciences.

References

[1] A. Hyvarinen and E. Oja, "A fast fixed-point algorithm for independent component analysis," *Neural Computation*, vol. 9, pp. 1483–1492, 1997.

[2] A. Hyvarinen, "A family of fixed-point algorithms for independent component analysis," in *Proc. of IEEE ICASSP'97*, 1997, pp. 3917–3920.

[3] M. Gaeta and J. L. Lacoume, "Source separating without prior knowledg: The maximum likelihood solution," in *Proc. of EUSIPCO'90*, 1990, pp. 621–624.

[4] P. Comon, "Independent componenet analysis, a new concept?" *Signal Proc.*, vol. 36, no. 3, pp. 287–314, 1994.

[5] A. Bell and T. Sejnowski, "An information-maximization approach to blind separation and blind deconvolution," *Neural Computation*, vol. 7, pp. 1129–1159, 1995.

[6] J. F. Cardoso and A. Souloumiac, "Blind beamforming for non-gaussian signals," *Radar and Signal Processing, IEE Proceedings F*, vol. 140, pp. 362–370, 1993.

[7] C. Jutten and J. Herault, "Blind separation of sources, part i : An adaptive algorithm based on neuromimetic architecture," *Signal Processing*, vol. 24, pp. 1–10, 1991.

[8] A. Belouchrani and J. F. Cardoso, "Maximum likelihood source separation for discrete sources," in *Proc. EUSIPCO 1994*, 1994, pp. 768–771.

[9] M. Zibulevsky, B. A. Pearlmutter, P. Bofill, and P. Kisilev, *Blind Source Separation by Sparse Decomposition, chapter in the book Independent Component Analysis: Principles and Practice*. Cambridge University Press, 2001.

[10] S. Zazo, Y. Blanco-Archilla, and L. Garcia, "Blind spatial multiplexing using order statistics for time-varying channels," in *Proc. of ICA2006*, 2006, pp. 414–421.

[11] W. Addison and S. Roberts, "Blind source separation with non-stationary mixing using wavelets," in *Proc. Of ICA2006*, 2006.

[12] K. E. Hild, D. Erdogmus, and J. C. Principe, "On-line minimum mutual information method for time-varying blind source separation," in *Proc. of ICA2001*, 2001, pp. 126–131.

[13] ——, "Blind source separation of time-varying, instantaneous mixtures using an on-line algorithm," in *Proc. of IEEE ICASSP'02*, 2002, pp. 993–996.

[14] A. B. Gharbi and F. M. Salam, "Algorithms for blind signal separation and recovery in static and dynamic environments," in *Proc. of IEEE ISCAS'97*, vol. 1, 1997, pp. 713–716.

[15] V. Koivunen, M. Enescu, and E. Oja, "Adaptive algorithm for blind separation from noisy time-varying mixtures," *Neural Comput.*, vol. 13, pp. 2339–2357, 2001.

[16] D. P. Mandic and A. Cichocki, "An online algorithm for blind extraction of sources with different dynamical structures," in *Proc. of ICA2003*, 2003, pp. 645–650.

[17] D. P. Mandic, A. Cichocki, and U. Manmontri, "An on-line algorithm for blind source extraction based on nonlinear prediction approach," in *Proc. of the IEEE Workshop on Neural Networks for Signal Processing, NNSP 2003*, 2003, pp. 429–438.

[18] P. Baxter, G. Spence, and J. McWhirter, "Blind signal separation on real data: Tracking and implementation," in *Proc. of ICA2006*, 2006, pp. 327–334.
[19] R. Everson and S. Roberts, "Non-stationary independent component analysis," in *Proc. ICANN 99*, vol. 1, 1999, pp. 503–508.
[20] ——, "Blind source separation for non-stationary mixing," *VLSI Signal Processing Systems*, vol. 26, pp. 15–23, 2000.
[21] ——, *Particle filters for nonstationary ICA. In Independent Component Analysis: Principles and Practice*. Cambridge University Press, 2001, pp. 280–298.
[22] M. Enescu and V. Koivunen, "Tracking time-varying mixing system in blind separation," in *Proc. Of Sensor Array and Multichannel Signal Processing Workshop*, 2000, pp. 291–295.
[23] H. Szu and I. Kopriva, "Deterministic blind source separation for space variant imaging," in *Proc. of ICA2003*, 2003, pp. 669–674.
[24] I. Kopriva and H. Szu, "Space-time variant blind source separation with additive noise," in *Proc. of ICA2004*, 2003, pp. 240–247.
[25] H. Szu and I. Kopriva, "Unsupervised learning with stochastic gradient," *Neurocomputing*, vol. 68, pp. 130–160, 2005.
[26] T. Weisman and A. Yeredor, "Separation of periodically time-varying mixtures using second-order statistics," in *Proc. of ICA2006*, 2006, pp. 278–285.
[27] A. Yeredor, "Tv-sobi: An expansion of sobi for linearly time-varying mixtures," in *Proc. of ICA2003*, 2003, pp. 903–908.
[28] L. Parra and C. Spence, "On-line blind source separation of non-stationary signals," *VLSI Signal Processing Systems for Signal Image and Video Technology*, pp. 39–46, 2000.
[29] R. Aichner, H. Buchner, S. Araki, and S. Makino, "On-line time-domain blind source separation of nonstationary convolved signals," in *Proc. Of ICA2003*, 2003, pp. 987–992.
[30] R. Aichner, H. Buchner, F. Yan, and W. Kellermann, "Real-time convolutive blind source separation based on a broadband approach," in *Proc. of ICA2004*, 2004, pp. 840–848.
[31] I. Kopriva, Z. Devcic, and H. Szu, "An adaptive short-time frequency domain algorithm for blind separation of nonstationary convolved mixtures," in *Proc. of IJCNN'01*, 2001, pp. 424–429.
[32] R. Mukai, H. Sawada, S. Araki, and S. Makino, "Robust real-time blind source separation for moving speakers in a room," in *Proc. of IEEE ICASSP'03*, vol. 5, 2003, pp. 469–472.
[33] ——, "Real-time blind source separation for moving speakers using blockwise ica and residual crosstalk subtraction," in *Proc. of ICA2003*, 2003, pp. 975–980.
[34] ——, "Blind source separation for moving speech signals using blockwise ica and residual crosstalk subtraction," *IEICE Trans. of Fundamentals of Electronics, Communications and Computer Sciences*, vol. E87-A, pp. 1941–1948, 2004.
[35] J. Anemüller and T. Gramss, "On-line blind separation of moving sound sources," in *Proc. of the ICA1999*, 1999, pp. 331–334.
[36] A. Koutvas, E. Dermatas, and G. Kokkinakis, "Blind speech separation of moving speakers in real reverberant environments," in *Proc. of IEEE ICASSP'00*, 2000, pp. 1133–1136.
[37] J. Anemuller and B. Kollmeier, "Adaptive separation of acoustic sources for anechoic conditions: A constrained frequency domain approach," *Speech Communication*, vol. 39, pp. 79–95, 2003.
[38] A. Yeredor, "Blind source separation in the presence of doppler frequency shifts," in *Proc. IEEE ICASSP'05*, vol. 5, 2005, pp. 277–280.
[39] D. Erdogmus, L. Vielva, and J. C. Principe, "Nonparametric estimation and tracking of the mixing matrix for underdetermined blind source separation," in *Proc. of ICA2001*, 2001, pp. 189–193.
[40] P. O'grady, B. Pearlmutter, and S. Rickard, "Survey of sparse and non-sparse methods in source separation," *IJIST*, vol. 15, no. 1, pp. 18–33, 2005.
[41] R. Kaftory, "Blind separation of time/position varying mixtures," *PhD. dissertation, Technion - Israel Institute of Technology*, 2009.
[42] B. Olshausen and D. Field, "Sparse coding with an overcomplete basis set: A strategy employed by v1?" *Vision Research*, vol. 37, pp. 3311–3325, 1997.
[43] J. P. Berrut and L. N. Trefethen, "Barycentric lagrange interpolation," *SIAM Rev*, vol. 46, pp. 501–517, 2004.
[44] F. Marvasti, *Random topics in nonuniform sampling, chapter in the book Nonuniform Sampling: Theory and Practice*. Kluwer Academic/Plenum Publishers, 2001, pp. 170–173.
[45] L. Zadeh, "Frequency analysis of variable networks," in *IRE Proc.*, vol. 38, 1950, pp. 291–299.
[46] H. Gafni and Y. Y. Zeevi, "A model for separation of spatial and temporal information," *Biol. Cybernetics*, vol. 28, pp. 73–82, 1977.
[47] H. D'Angelo, *Linear Time-Varying Systems: Analysis and Synthesis*. Allyn and Bacon, 1970.
[48] R. kaftory and Y. Y. Zeevi, "Probabilistic geometric approach to blind separation of time-varying mixtures," in *Lecture Notes in Computer Science: Independent Component Analysis and Signal Separation*, vol. 4666, 2007, pp. 373–380.
[49] P. Kisilev, M. Zibulevsky, and Y. Y. Zeevi, "A multiscale framework for blind source separation," *J. of machine learning research*, vol. 4, pp. 1339–1363, 2003.
[50] D. Ballard, "Generalizing the hough transform to detect arbitrary shapes," *Pattern Recognition*, vol. 13(2), pp. 111–122, 1981.
[51] D. Scott, *Multivariate density estimation: Theory, Practice, and Visualization*. Wiley, 1992, p. 139.
[52] R. Kaftory and Y. Y. Zeevi, "Blind separation of images obtained by spatially-varying mixing system," in *Proc. IEEE ICIP 08*, 2008, pp. 2604–2607.
[53] ——, "Blind separation of position varying mixed images," in *Proc. IEEE ICIP 09*, 2009.
[54] M. Oren and S. K. Nayar, "A theory of specular surface geometry," in *Proc. IEEE ICCV*, 1995, pp. 740–747.
[55] D. G. Lowe, "Object recognition from local scale-invariant features," in *Proc. IEEE ICCV*, 1999, pp. 1150–1157.
[56] N. Sochen, R. Kimmel, and R. Malladi, "A general framework for low level vision," *IEEE Trans. IP*, vol. 7, pp. 310–318, 1998.
[57] A. M. Polyakov, "Physics letters," vol. 103B, p. 207, 1981.
[58] R. Kimmel, R. Malladi, and N. Sochen, "Images as embedded maps and minimal surfaces: Movies, color, texture and volumetric medical images," *Int. J. Comp. Vision*, vol. 39, pp. 111–129, 2000.
[59] R. Kaftory, "Color image restoration using the beltramy framework," *MSc. dissertation, Technion - Israel Institute of Technology*, 2002.
[60] R. Kaftory, N. Sochen, and Y. Zeevi, "Variational blind deconvolution of multi-channel images," *Int. J. Imag. Science and Tech.*, vol. 15, pp. 56–63, 2005.

[61] C. Vogel and M. Oman, "Iterative methods for total variation denoising," *SIAM J. of Scientific Computing*, vol. 17, pp. 227–238, 1996.
[62] R. Kaftory, Y. Y. Schechner, and Y. Y. Zeevi, "Variational distance-dependent image restoration," in *Proc. IEEE CVPR*, 2007.

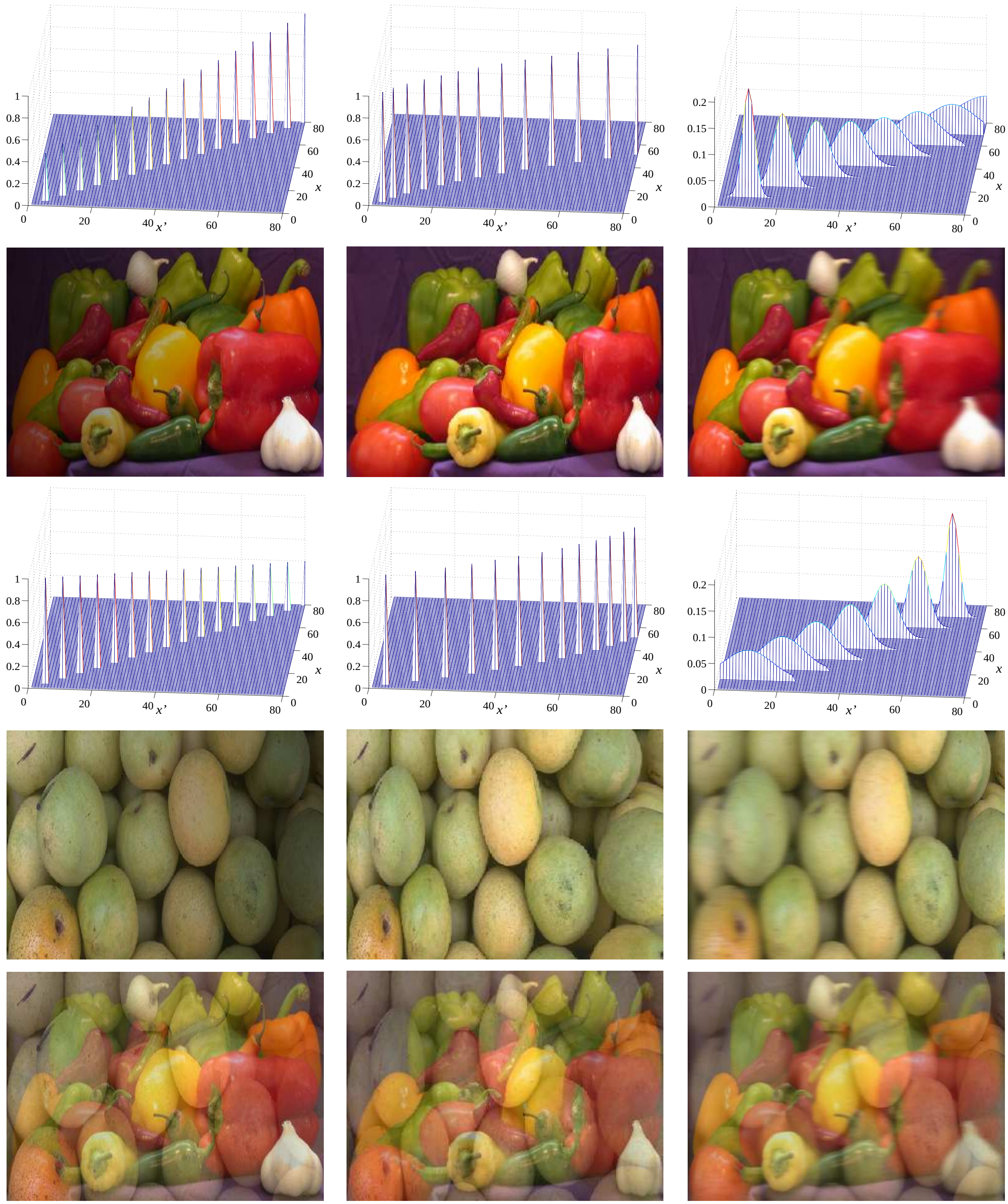

Fig. 1. Types of position varying image mixtures, where the system varies only along the x axis. Left column: instantaneous case. Middle column: single-path case. Right column: multi-path case. From top to bottom: mixing filter $h_{11}(x, x')$, result of filtering one of the sources with this filter, mixing filter $h_{12}(x, x')$, result of filtering the other source with this filter, the mixture. Observe how the following property of the filtered image changes along the x axis: intensity for the instantaneous case, scale for the single-path case and blur for the multi-path case.

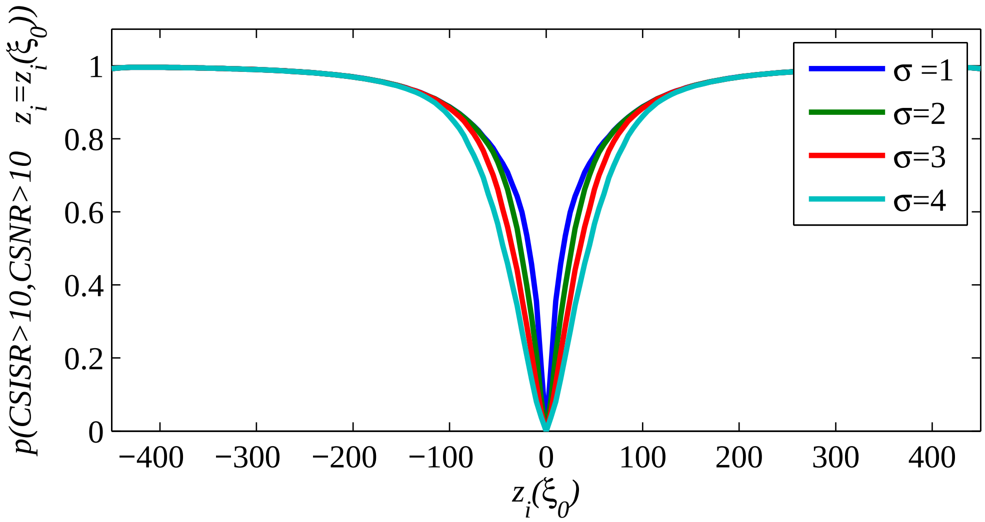

Fig. 2. The conditional probability that one source is active and the other is not (and the noise is negligible), given the thresholds th_1, th_2 and the observed mixture plotted for several values of σ, given sparse signal distribution with $\mu = 1.5$ and $\nu = 2$. Observe how the probability is a symmetric non decreasing function.

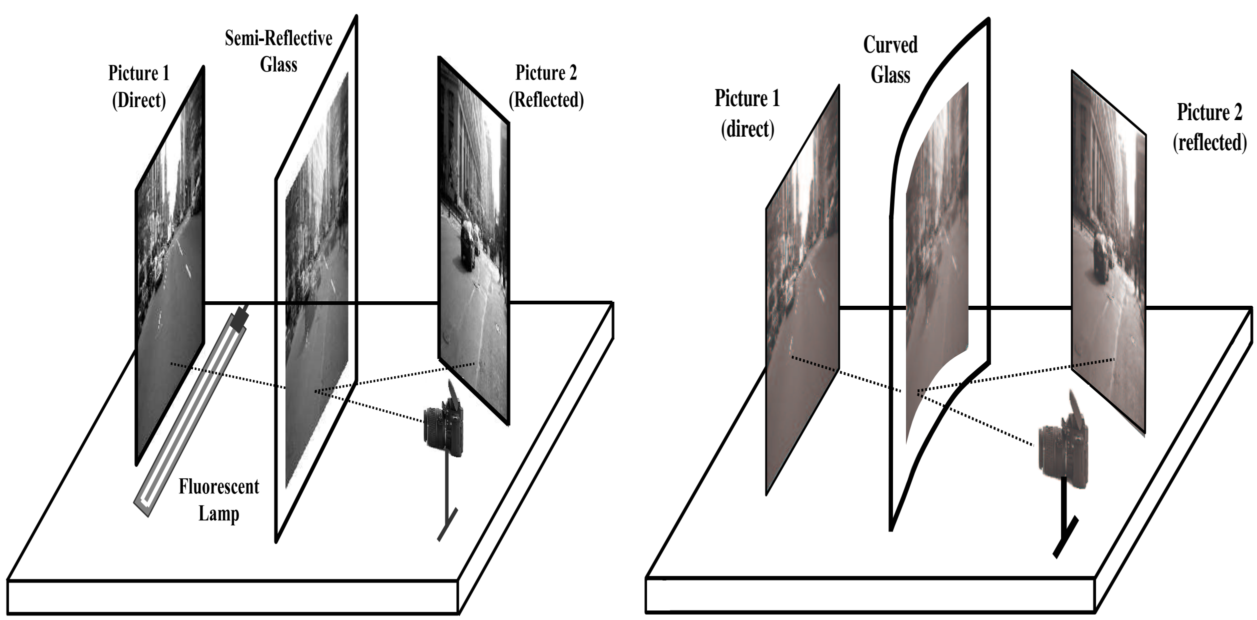

Fig. 3. An optical system generating spatial varying instantaneous mixtures (left) and spatial varying single-path mixtures (right): two pictures are positioned opposite to each other while a semi-reflective glass is mounted along the optical axis of one of them. In the case of instantaneous mixtures, the first mixture is generated using a uniform lighting. A second mixture is generated using a non-uniform illumination. In the case of single-path mixtures, the first and second mixtures are acquired from slightly different camera position

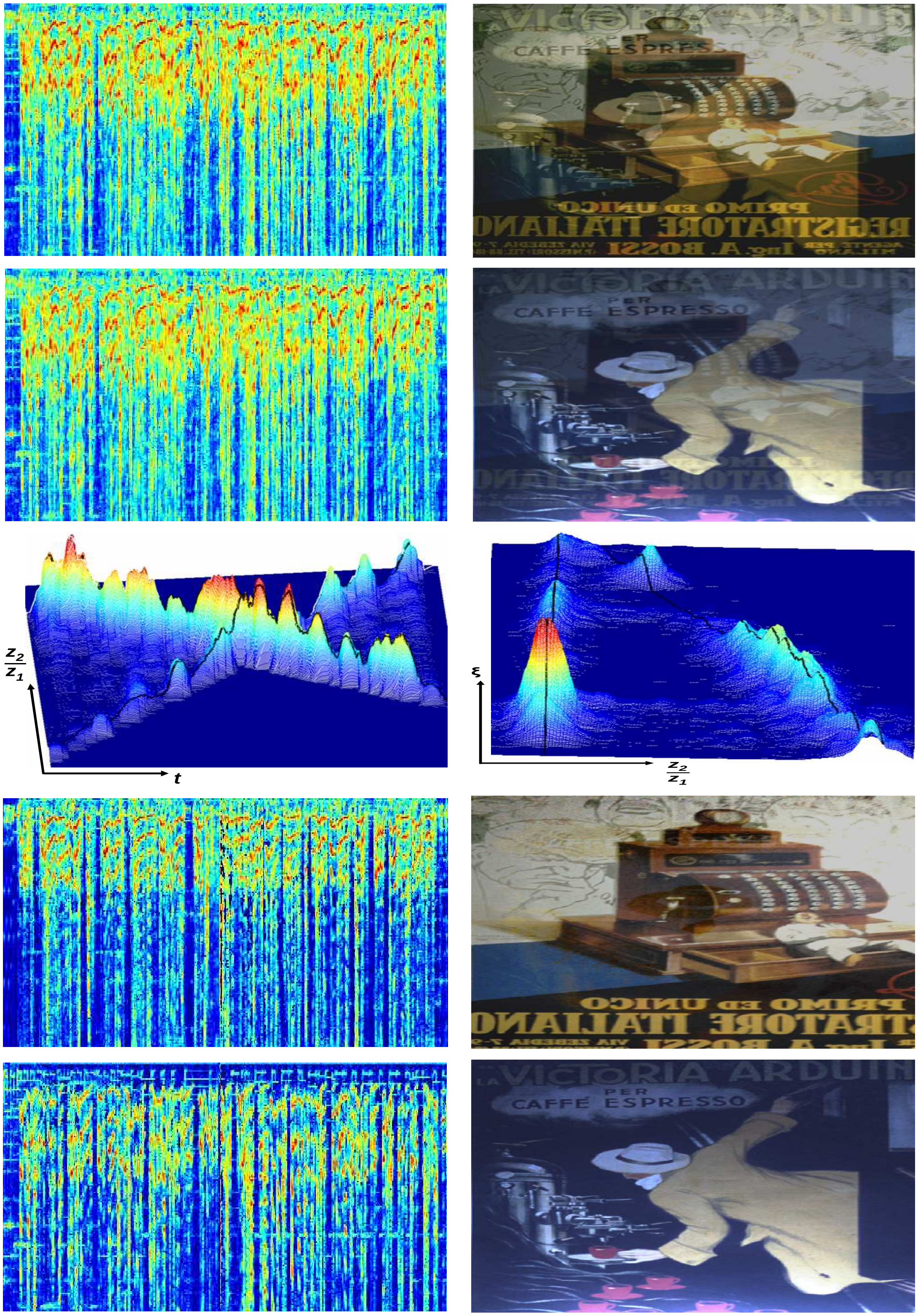

Fig. 4. [Left] Two audio signals of a man and a women voices are mixed. [Top left] The spectrograms of the two audio mixtures. [Middle left] Kernel-estimated probability density. The black lines indicates the estimated curves $g_i(\alpha_{i_k};\xi)$. [Bottom left] The spectrograms of the estimated separated sources. [Right] Mixtures produced by the setup depicted on the left in Fig. 3. [Top right] A mixture of the images obtained in room lighting and with the addition of non-uniform lighting to the transmitted image. [Middle right] Kernel-estimated probability density. The black lines indicate the estimated curves $g'_i(\alpha_{i_k};\xi)$. [Bottom right] The estimated image sources.

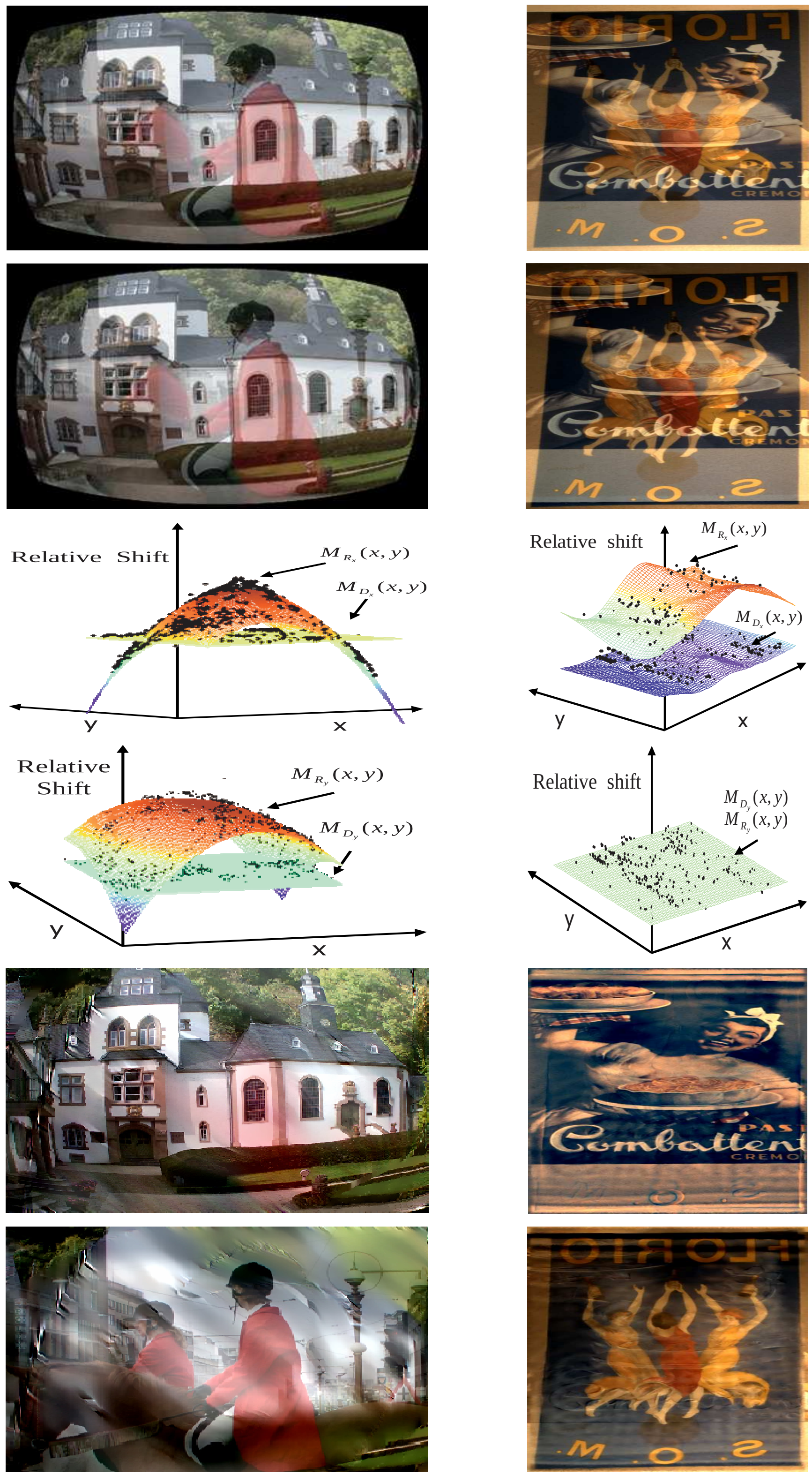

Fig. 5. Simulated (left) and experimental (right) single-path image mixtures obtained by a round semi-reflector. [Top] Image mixtures. [Middle] Estimated surfaces obtained by surface fitting of matching SIFT keypoints. [Bottom] The estimated image sources.

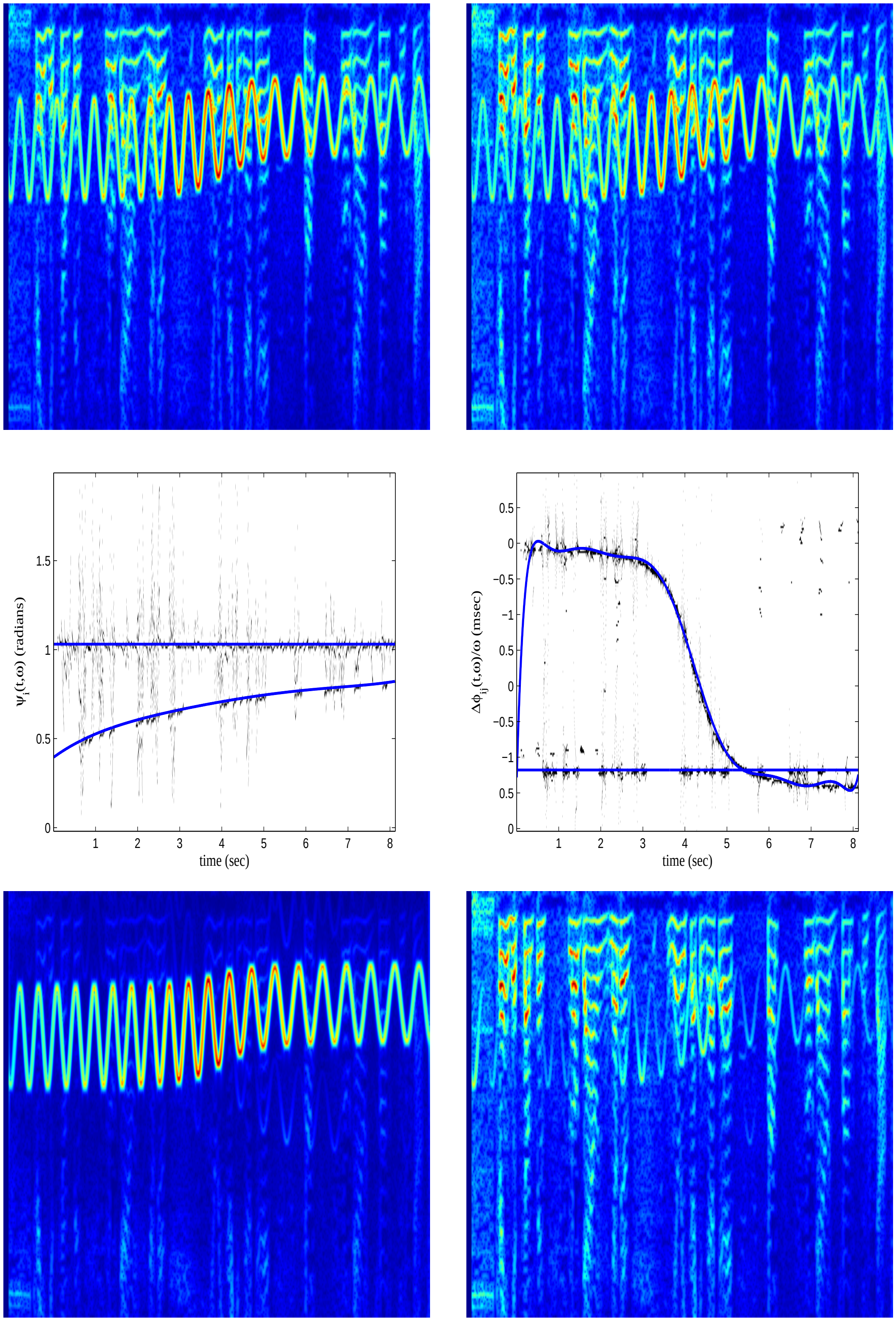

Fig. 6. An audio signal of a man's voice is mixed with the sound of a siren generated according to a semi-realistic scenario. [Top] The spectrograms of the two audio mixtures. [Middle] The amplitude and phase of the mixing filters. [Bottom] The spectrograms of the estimated separated sources.